STYRELSEN FÖR

VINTERSJÖFARTSFORSKNING

WINTER NAVIGATION RESEARCH BOARD

Research Report No 28

LONG TERM MEASUREMENTS OF ICE PRESSURE AND ICE-INDUCED STRESSES ON THE ICEBREAKER SISU IN WINTER 1978

J. VUORIO, K. RISKA, P. VARSTA

Sjöfartsstyrelsen
Finland

Finnish Board of Navigation

Sjöfartsverket
Sverige

Swedish Administration
of Shipping and Navigation

J. Vuorio, K. Riska, P. Varsta

LONG-TERM MEASUREMENTS OF ICE PRESSURE AND ICE-INDUCED STRESSES ON THE ICEBREAKER SISU IN WINTER 1978

ISBN 951-46-3979-0

F O R E W O R D

The Winter Navigation Research Board presents its report no 28. This report can be seen as a continuation to the report no 21. The aim is to obtain more accurate information about the ice pressure and ice inducedt stresses on the hull of a ship and thus provide a better basis for the determination of hull scantlings for ice strengthened ships. The Winter Navigation Research Board expresses its thanks to the research team, the personnel of the ice breaker SISU and others who have contributed to this work.

Helsingfors and Stockholm April 1979

Jan-Erik Jansson Lennart Johansson

CONTENTS

1. INTRODUCTION

The aim of this report is to obtain relevant data for the dimensioning procedure of the shell structure of an ice-going vessel in the Baltic. The dimensioning ice loads have formerly been obtained by indirect methods because there is a lack of reliable analytical models of ice pressure and load and because so far empirical data of them is not available.

The only values published about ice loads are calculated indirectly from the response of the shell structure. The response is measured with strain gauges. This method does not give the value of ice pressure or load area, only an estimate of the total load. Thus it was decided to design a measuring system for local ice pressure.

Nowadays practically all the estimates of dimensioning loads for various structures are of stochastic nature. Also the ice load is a stochastic variable and to investigate its characteristics a special recording system was developed.

This system was in operation onboard the Finnish icebreaker SISU during winter 1978. In this winter the output of four gauges was analysed. These gauges included two V-shaped strain gauges on the plating and two new ice pressure gauges. The measuring period was from 24.2. to 7.5. 1978. During this time the icebreaker was operating in the Bothnian Bay mainly from Kemi.

2. MEASURING SYSTEM

2.1 Icebreaker SISU

The main dimensions of the Baltic icebreaker SISU are the following:

length, max	104.6 m
length, DWL	96.0 m
breadth, max	23.8 m
breadth, DWL	22.5 m
draught, max	8.3 m
draught, DWL	7.3 m
power	16.2 MW
speed in open water	18.7 knots

The shell structure of the icebreaker SISU consists of plating, frames (s = 400 mm), horizontal stringers and webframes (s = 2400 mm). The frames are perpendicular to the symmetry plane of the ship.

In fig. 1 is the side view of the icebreaker SISU showing also the area where the transducers were located.

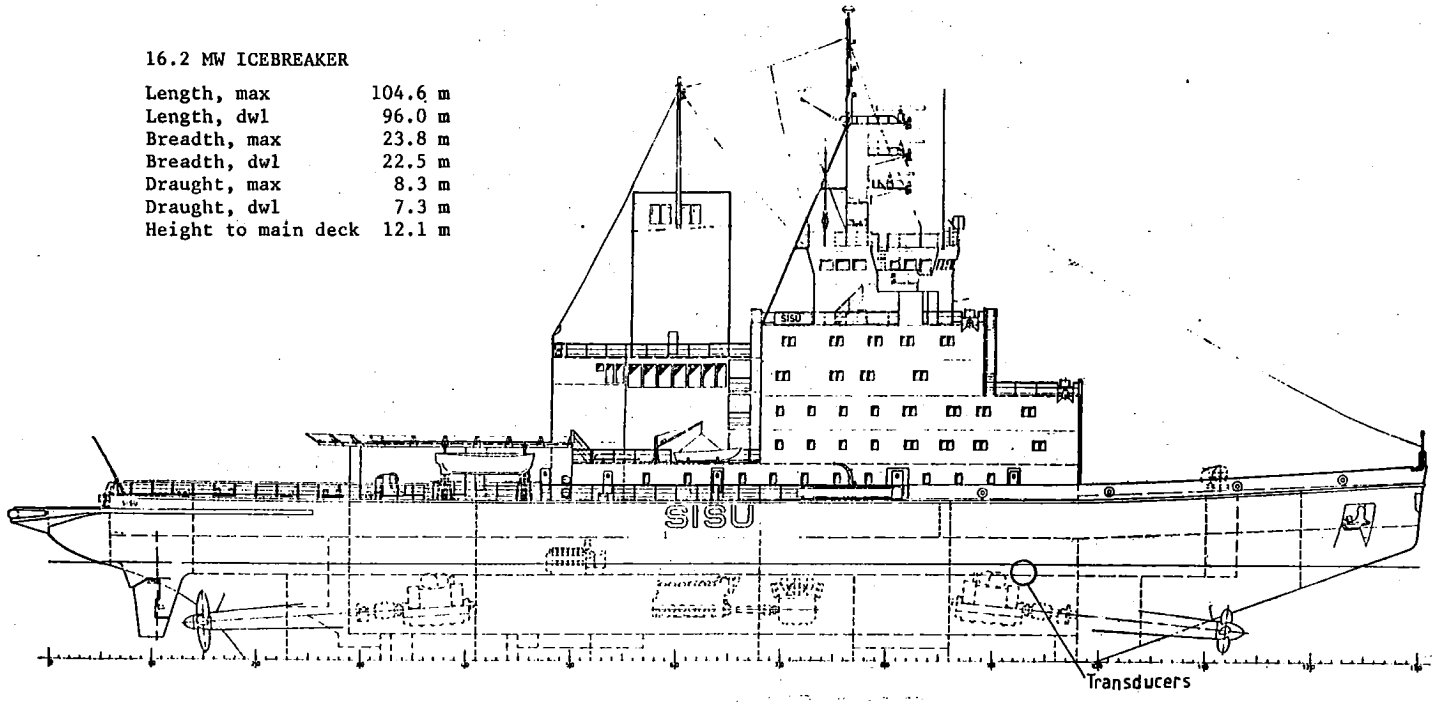

Fig. 1. Side view of the Baltic icebreaker SISU.

2.2 Data collecting system

An automatic microprocessor-based data collecting system was developed for the ice pressure measurements. The scheme of the measuring system is shown in fig. 2. It is possible to attach 8 transducers to the system, but only 5 were used in winter 1978. The sampling of the transducer signals was made by a Hewlett-Packard digital voltmeter equipped with a scanning unit. The sampling frequency was 1000 Hz, which means 125 samples per second per channel.

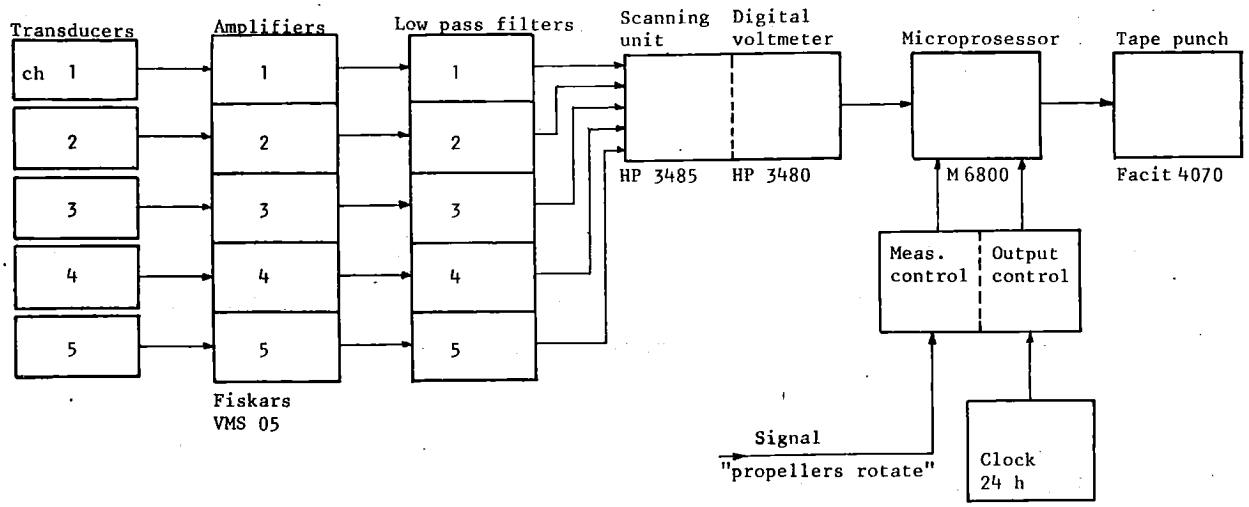

Fig. 2. Scheme of the measuring system.

The signal level distributions for each channel were formed by means of a microprocessor, which divides each sample in one of 20 classes according to the amplitude and adds one count in corresponding memory register.

The measurement commences when one of the aft propellers starts to rotate in forward direction and is interrupted after a 15 second delay when both of the aft propellers are stopped. The distributions

were punched on paper tape once a day at midnight. The memory of the microprocessor was secured against an electrical breakdown by means of accumulators.

A photograph of the data collecting system is shown in fig. 3. An example of the print-out of the system is presented in fig. 4.

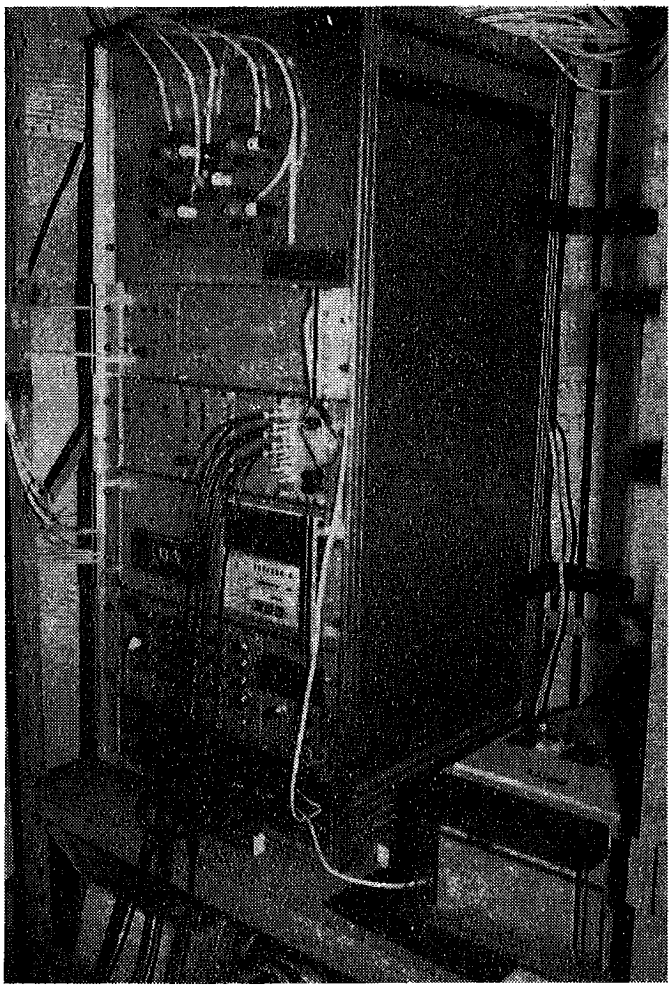

Fig. 3. The data collecting system.

```
a)
71
b) c) d)
1 00 00000000
1 01 00001425
1 02 08031887
1 03 00014322
1 04 00002720
1 05 00000850
1 06 00000311
1 07 00000092
1 08 00000046
1 09 00000013
1 10 00000013
1 11 00000007
1 12 00000004
1 13 00000002
1 14 00000000
1 15 00000000
1 16 00000000
1 17 00000000
1 18 00000000
1 19 00000000
```

a) No. of record (day)
b) No. of channel
c) Class
d) Samples in class

Fig. 4. An example of a print-out of the data collecting system.

2.3 Ice pressure gauges

Two specially designed ice pressure gauges were mounted on the shell of the ship. When designing the ice pressure gauge, the following aspects were to be considered:

- On the shell surface outside the pressure gauge no discontinuities whatever are allowed because they may affect the breaking process of ice.
- The gauge is not allowed to cause any risks for the safety of the ship by reducing the strength of the shell structure.

For these reasons any holes in the plating are out of question. For the operation of the gauge, the following demands are to be fullfilled:

- The gauge must have sufficient sensitivity and linearity.
- The gauge may not be sensitive to the variations of the area of ice pressure, i.e. it shall measure only the local pressure.

The principle of the gauge is to measure the deflection of a restricted area of the shell plating caused by ice pressure. The surroundings of that area (Ø 200 mm) are well stiffened by the thick steel cover of the gauge, and the brackets shown in fig. 5. The sensing element of the gauge is realized using the strain gauge technique. In connection with the pressure gauge PG1, an alternative realization of the pressure gauge was studied. A strain gauge bridge was mounted directly on the plating (PG1A). The outputs of the strain gauge bridges were amplified by a Fiskars DC-amplifier. A photograph of a pressure gauge mounted is shown in fig. 5.

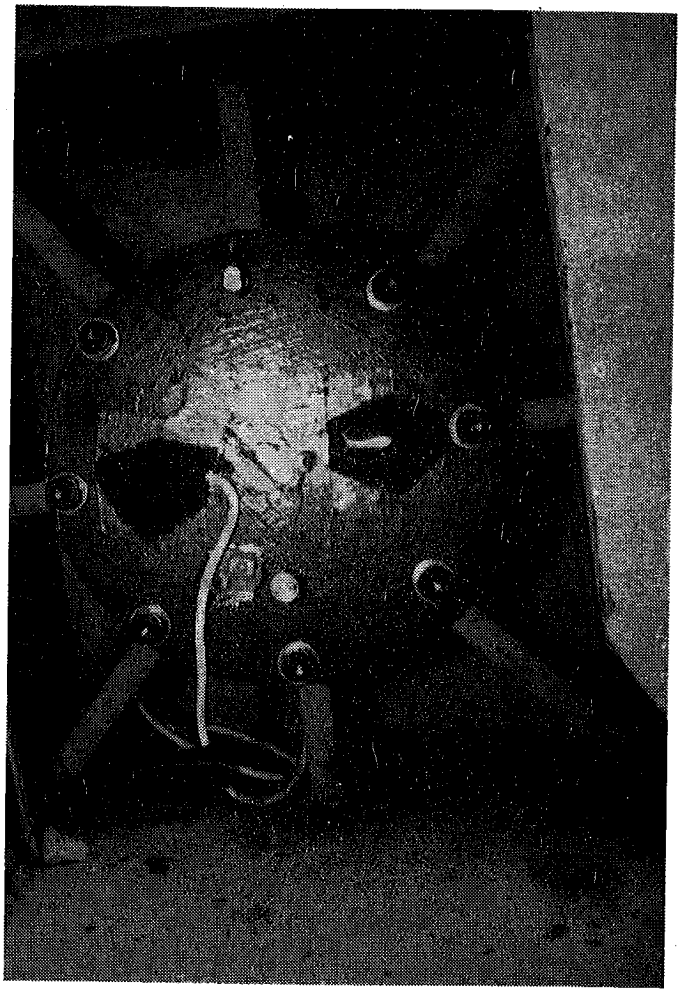

Fig. 5. The ice pressure gauge mounted.

The location of the gauges is shown in fig. 6. The heights from the base line of the gauges were 6.71 m (PG1) and 7.21 m (PG2). During the winter 1977 the locations were based on the mean draught of the ship, which was 7.61 m at frame 94 according to the logbook of the ship. In 1978 this mean draught was also 7.61 m the minimum being 7.35 m and the maximum 7.85 m.

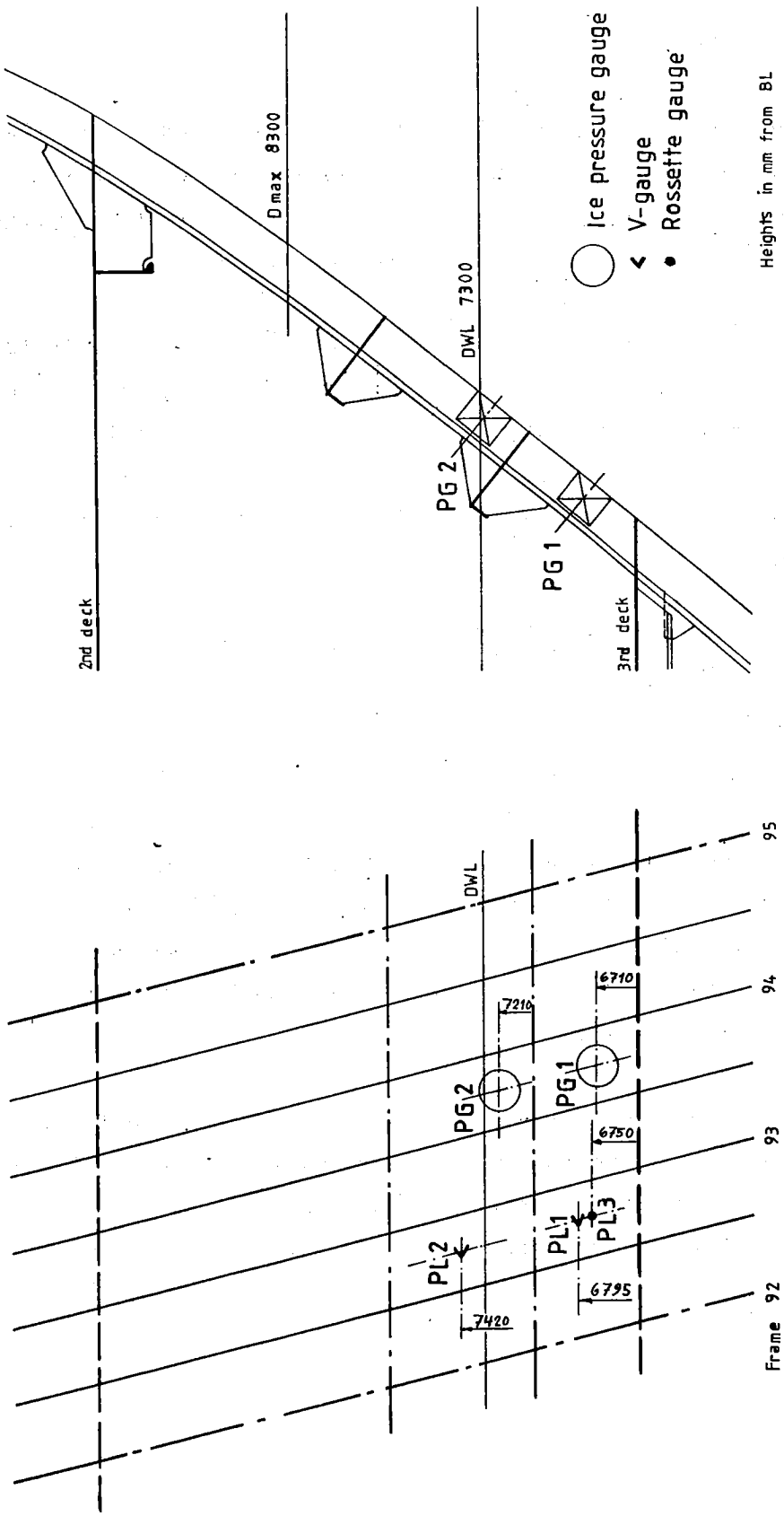

Fig. 6. Location of transducers.

2.4 Strain gauges

Two V-shaped strain gauges (PL1 and PL2) were mounted on the shell plating, in the midpoint of an area restricted by two frames and two stringers. The angle between the two elements in the V-gauge was 56^{o} and the measuring direction was horizontal.

To check the directions of the principal stresses also a 3 x 120^{o} Rossette gauge (PL3) was mounted in the vicinity of the V-gauge PL1. This measuring point was not connected to the statistical measuring system, but some time-histories were recorded by a tape recorder. The analysis showed that the direction of the bigger principal stress was horizontal, as assumed.

Locations of the strain gauges are also shown in fig. 6.

2.5 Calibration of the ice pressure gauges

Both of the two ice pressure gauges were calibrated by an internal hydraulic pressure up to 5 MN/m^2. The upper gauge (PG2) was calibrated also by external pressure up to 5 MN/m^2 and by external point force up to 130 kN corresponding to about 10 MN/m^2 uniform pressure on the area of the pressure gauges.

For the calibration by external hydraulic pressure a steel plate of dimensions 400 x 450 mm^2 was welded parallel to the shell plating 30 mm away from it, thus forming a kind of a pressure vessel. Fig. 7 is a photograph presenting the calibration with this method.

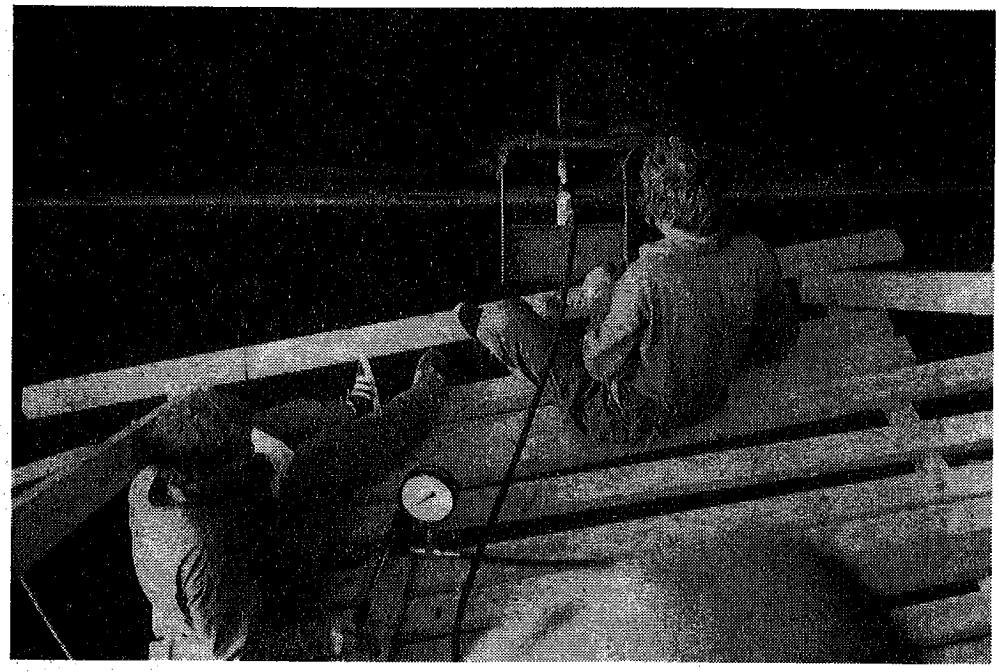

Fig. 7. Calibration by external pressure.

The calibration with an external point force was made by means of a hydraulic cylinder and a beam supported outside the frames as fig. 8 shows. The place of the pressure gauge was found roughly with an ultrasonic plate thickness meter, and after that exactly by pressing systematically the plate at different points and finding the place which gives the maximum output voltage.

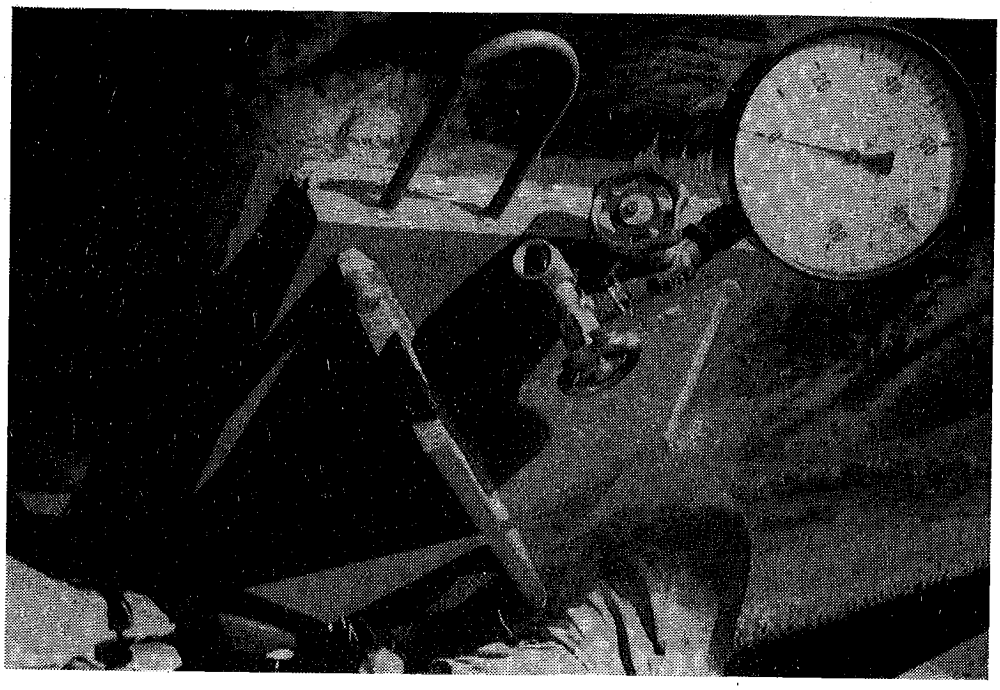

Fig. 8. Calibration by external point force.

The conversion from the point force to the uniform pressure was based on a FEM-model made to describe the pressure gauge and its environments. Fig. 9 shows the element mesh used. The results obtained from the FEM-model were in agreement with those obtained from the calibrations,as fig. 10 shows.

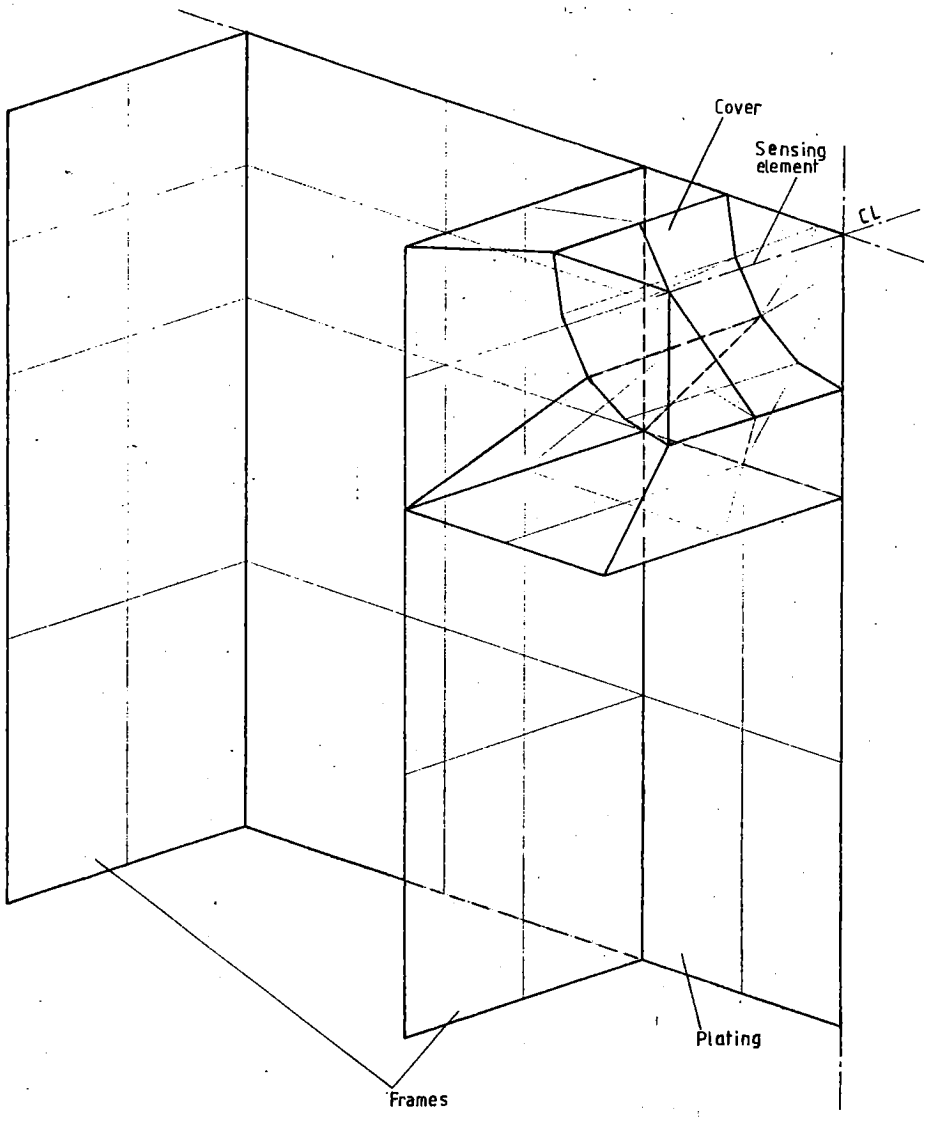

Fig. 9. The element mesh used in the FEM-calculations.

The linearity of the gauge was high in all the three calibration methods. The slopes of the calibration lines differ on the other hand much from each other. In the case of calibration with external pressure, this is caused by the reaction forces induced to the shell structure by the calibration plate. In the case of the internal pressure, the loading configuration is different and also the deformation of the cover may cause error in the display of the gauge. This is inconvinient because the internal calibration is technically much easier than the external methods. However, if it is possible to prove that the ratio between the slopes remains always constant, the internal calibration may be used at least when the external calibration is technically impossible.

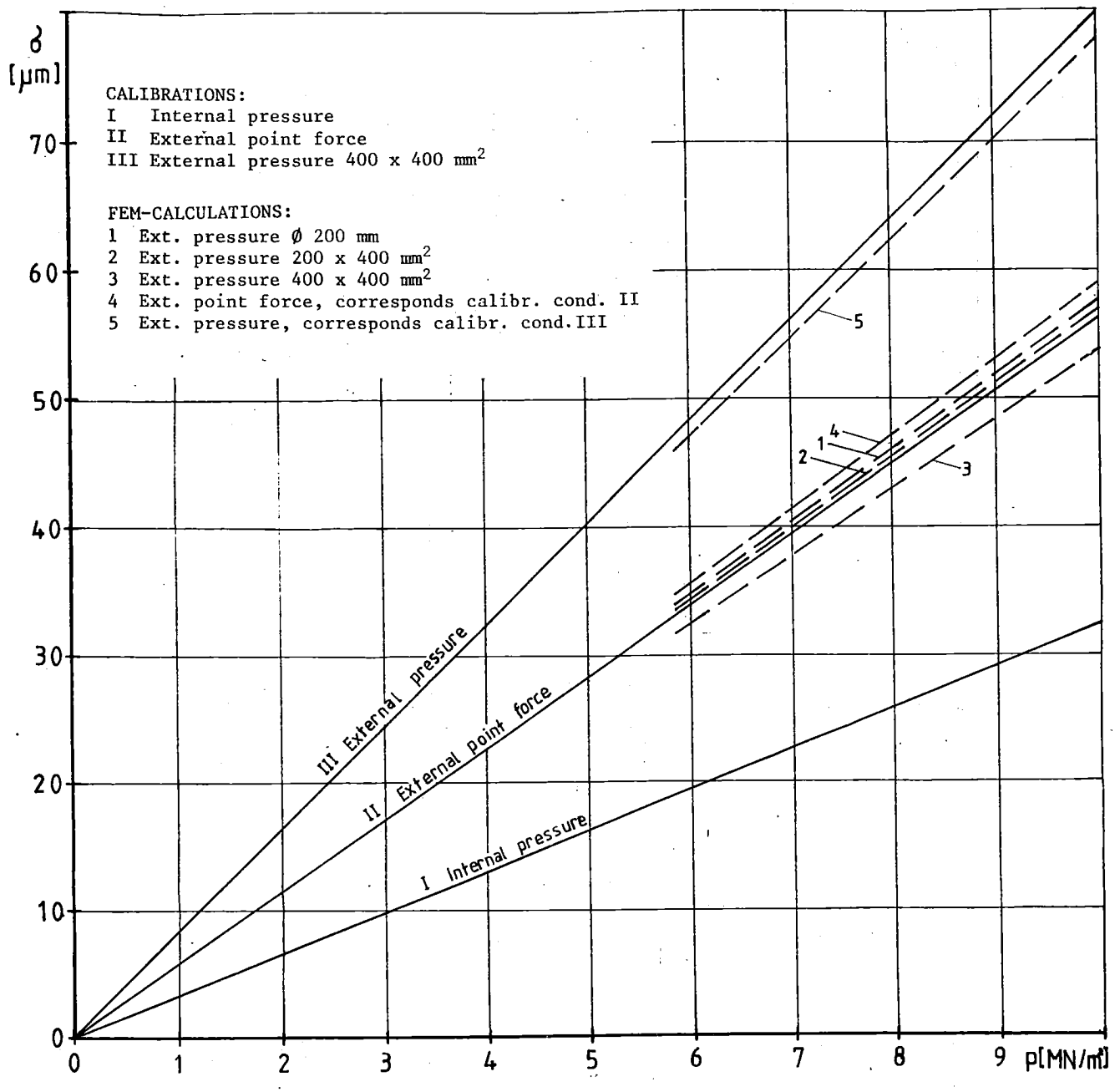

Fig. 10. The calibration lines obtained by various methods.

When simulating the different calibration methods by the FEM-model, the results showed the same tendency as the calibrations. On the basis of this examination it was obvious that the calibration with external point force gives the most reliable results and it has been used in the following analysis.

The FEM-calculations (cases 1 to 3) show also that the gauge has a low sensitivity to variations of the total force, which causes variations in the global displacement of the shell structure around the gauge. This is due to the stiffness of the surroundings of the gauge. In the icebreaker SISU the situation may be better than in the model because the gauges are located beside a stringer or a deck (225 mm from the centre of the gauge), whereas in the model this distance is 1200 mm. Thus the environments of the gauges are quite stiff and so the global displacement of the shell structure is small.

3. WINTER 1978

3.1 Overall description

The severity of the winter 1978 was about the average. The largest extension of the ice field was reached around 23.2., the amount of ice area being 170 000 km , fig. 11. In an average winter the ice area is about 184 000 km /6/. The ice conditions before this date are not of interest here because these measurements began on 24.2. In fig. 11 there is given also the approximate operation area of the icebreaker SISU during the measurement period.

After the date of maximum extent, the ice cover retreated somewhat and remained thereafter constant up till mid-April. During this time the ice cover in the Bothnian Bay was quite inhomogeneous, usually consisting of compact pack ice and ridged level ice. The ice cover in the Bothnian Bay can also be separated into two zones; landfast ice which is motionless and thus is not ridged, and ridged level ice. When open pack ice appeared it was between these two zones. The thickness of ice in the landfast zone was around 70 cm and in the level ice zone up to 50 cm. At the end of April the ice cover started to melt, which was also noticed by the formation of numerous leads. The ice cover disappeared finally in the end of May.

The advancement of ice winter can be examined in view of the daily averages of temperature along the coast of the Bothnian Bay, fig. 12. It is clearly noticed that the advance of ice cover ceased due to a rise of temperature up to around $0^{o}C$ for about 10 days. Because the temperature is the main variable affecting the advance of ice cover, it has a very large indirect influence on the ice loads by affecting the time ships must sail in ice.

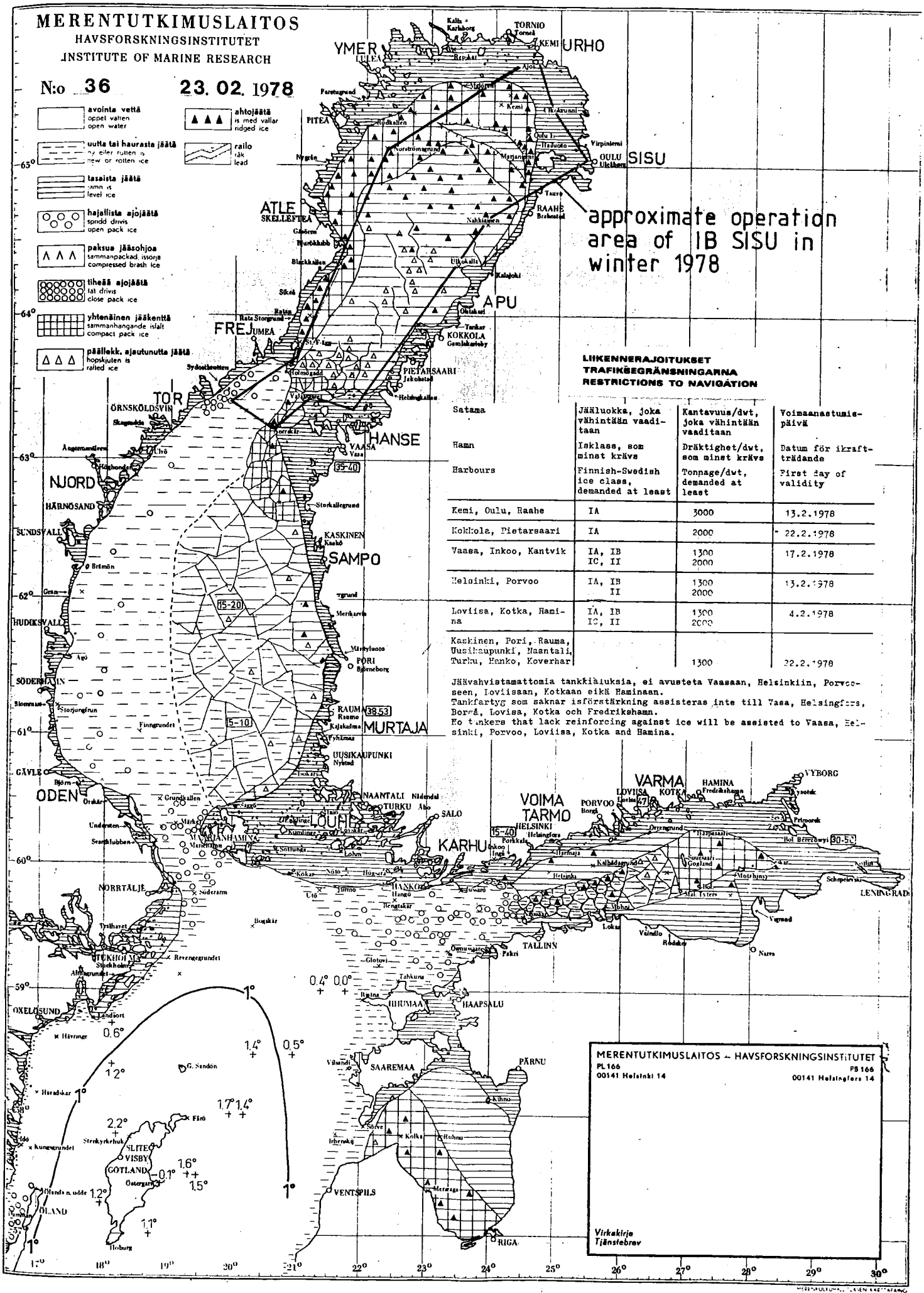

Fig. 11. The largest extension of ice during winter 1978.

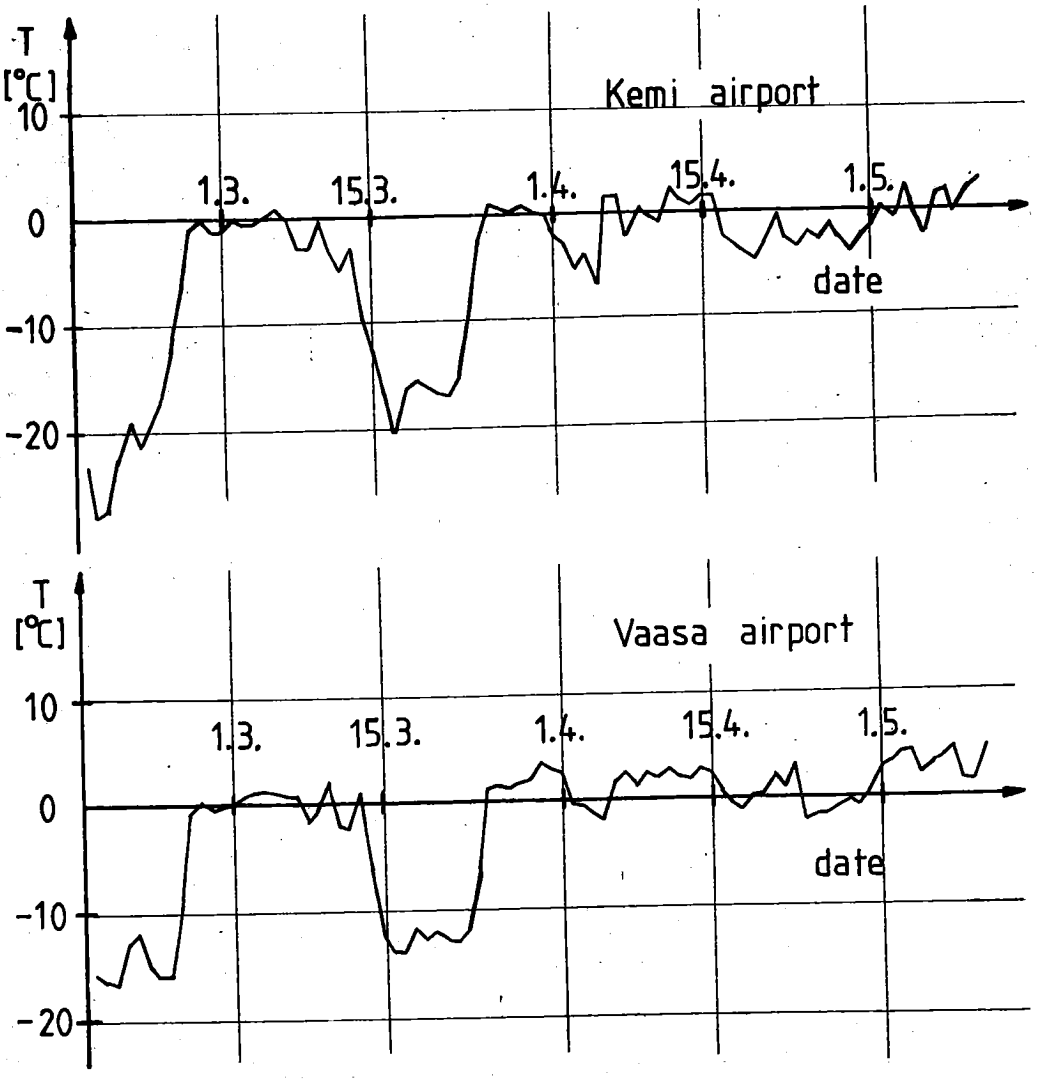

Fig. 12. Daily averages of air temperature during February - May 1978 in Kemi and Vaasa.

3.2 Special features of the ice conditions

For future reference some features of the ice situation influencing ice loads are described. The first factor is the ice thickness as a function of time. In fig. 13 there is depicted the ice thickness versus time in the landfast ice zone close to Oulu. It can be seen that the thickness remained almost constant during the measurement period.

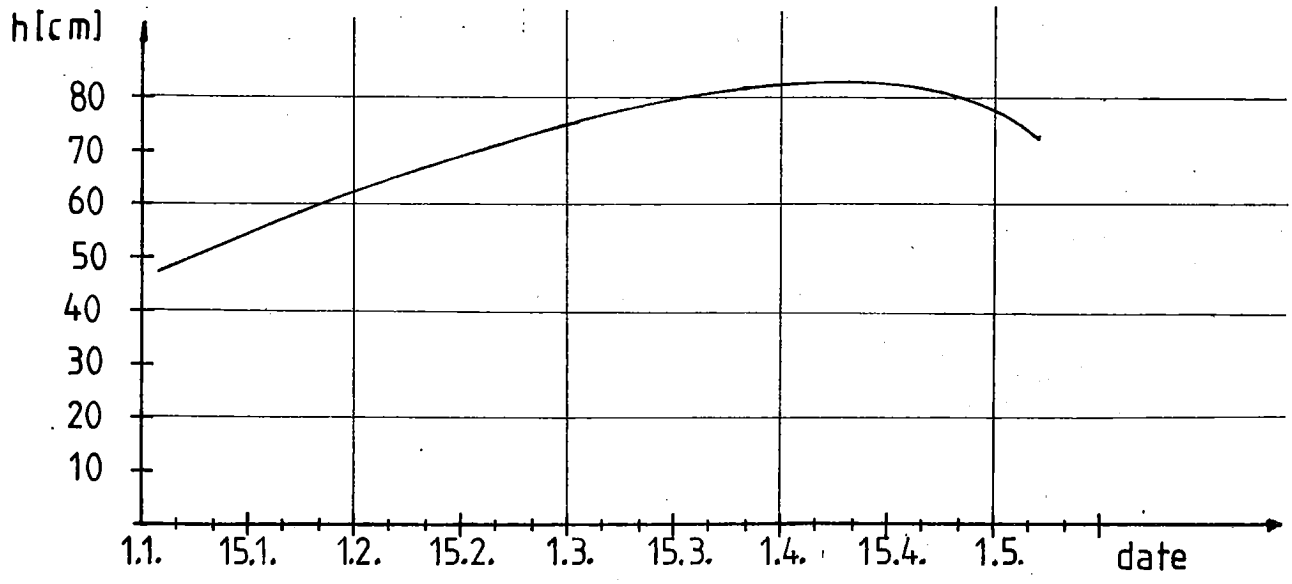

Fig. 13. Ice thickness close to Oulu in the winter 1978.

Another factor influencing the ice loads is the extent and location of leads along the Finnish coast. These make it possible for ships to navigate in open water. The first big lead which aided shipping in the Bothnian Bay was formed about 25.2., see fig. 14a. The lead remained open up to 10.3. From around 20.4. there was a zone of open pack ice between the landfast ice and level ice in the Bothnian Bay, fig. 14b.

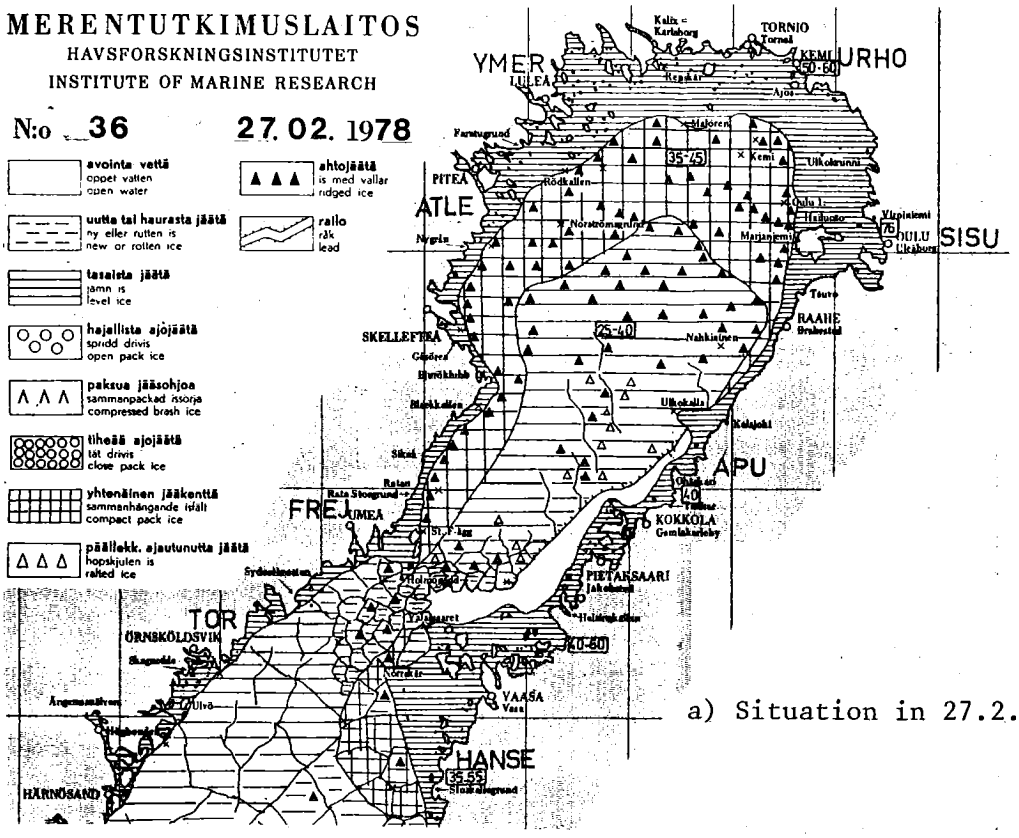

a) Situation in 27.2.

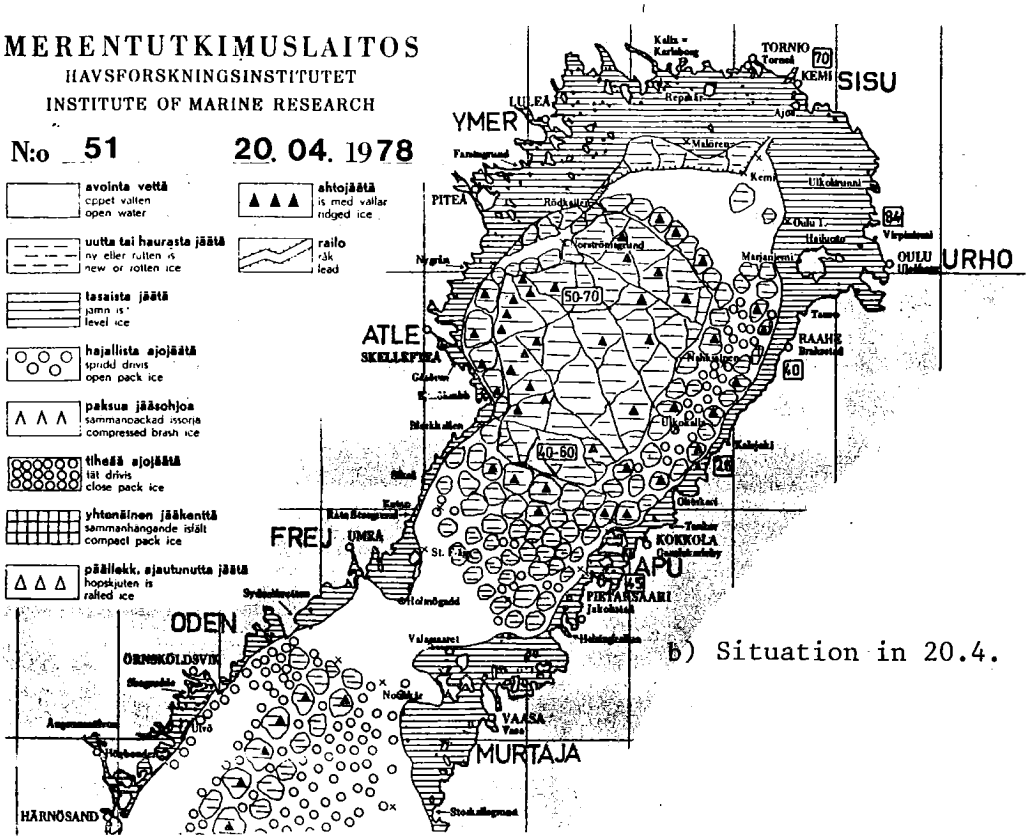

b) Situation in 20.4.

Fig. 14. Ice situation in the Bothnian Bay showing the main leads.

4. RESULTS OF MEASUREMENTS

4.1 Daily maxima

The main results of this investigation are the daily maxima of ice pressure and stress, see Appendix 1. These form the basis for statistical analysis from which relevant data of extreme ice pressure can be extrapolated. The daily maximum peak of stress or pressure can be a very isolated event; perhaps it does not even represent the prevailing ice conditions but is an outcome of some exceptional extremal situation. Thus the average value of, say, the 100 highest values corresponds better to the ice conditions the icebreaker is navigating in.

The daily maxima of ice pressure (PG1) and stress (PL1 and PL2) are presented in fig. 15a---c. Also the average of the 100 highest pressure or stress levels are depicted. The results of PG2 are not given because they are not reliable due to difficulties with the amplifier.

Between 21.4. and 27.4. icebreaker SISU was mainly standing still so no recordings were made during that time. The distributions of daily maxima with the calculated Gumbel-distributions are shown in fig. 16.

It can be seen from fig. 15 that the maximum daily value represents well the prevailing ice conditions because there is a close correlation between the maxima and the average of the 100 highest values. There are, however, a couple of exceptions. In PG1, for example, the maximum value is much higher than the preceding or following value in 23.3. and 11.4. but the averaged value does not deviate at all from the heighbouring values. Nevertheless these kinds of days are very few and they do not affect the statistical analysis which follows.

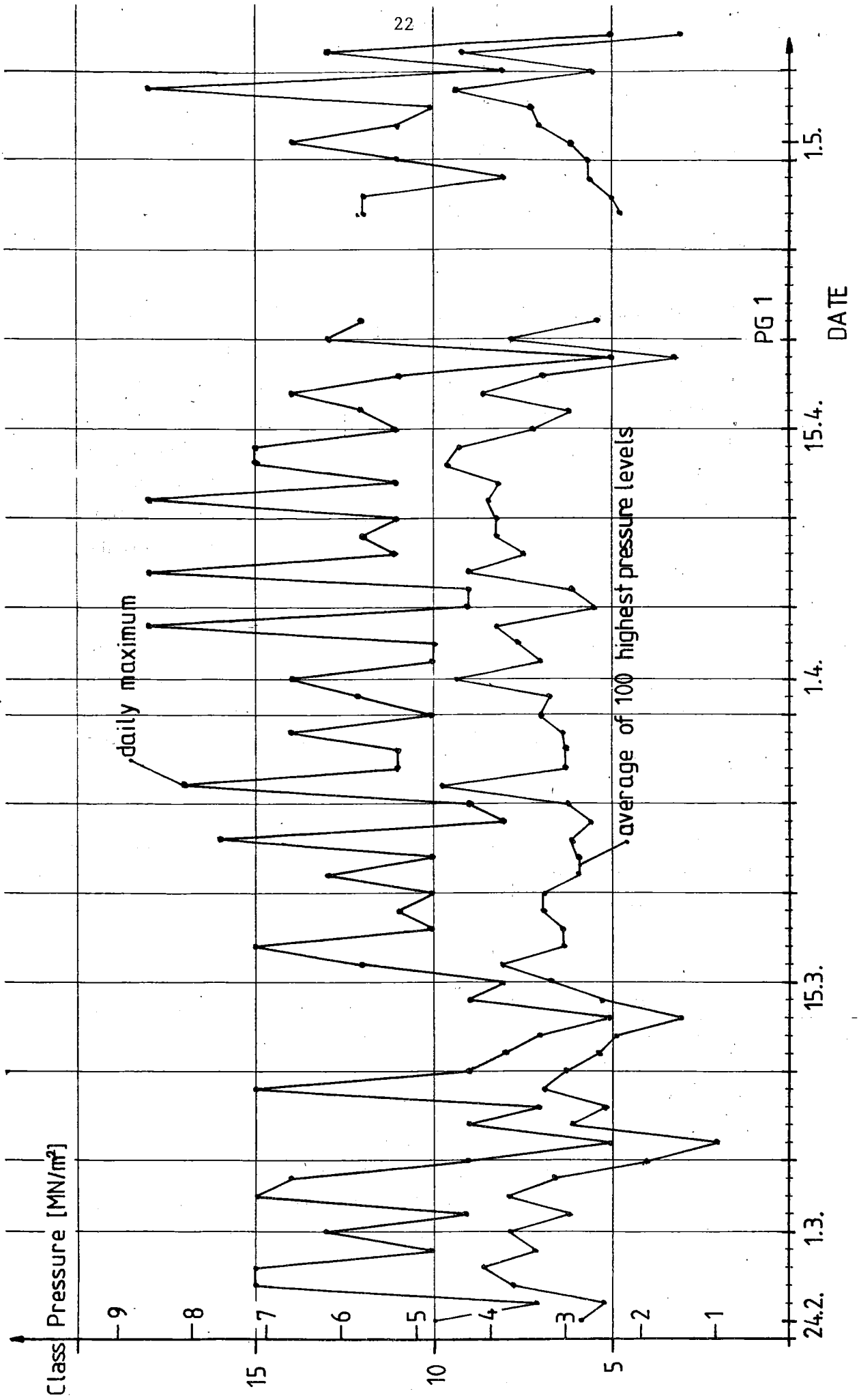

Fig. 15a. The daily maxima of PG1 during the measuring period.

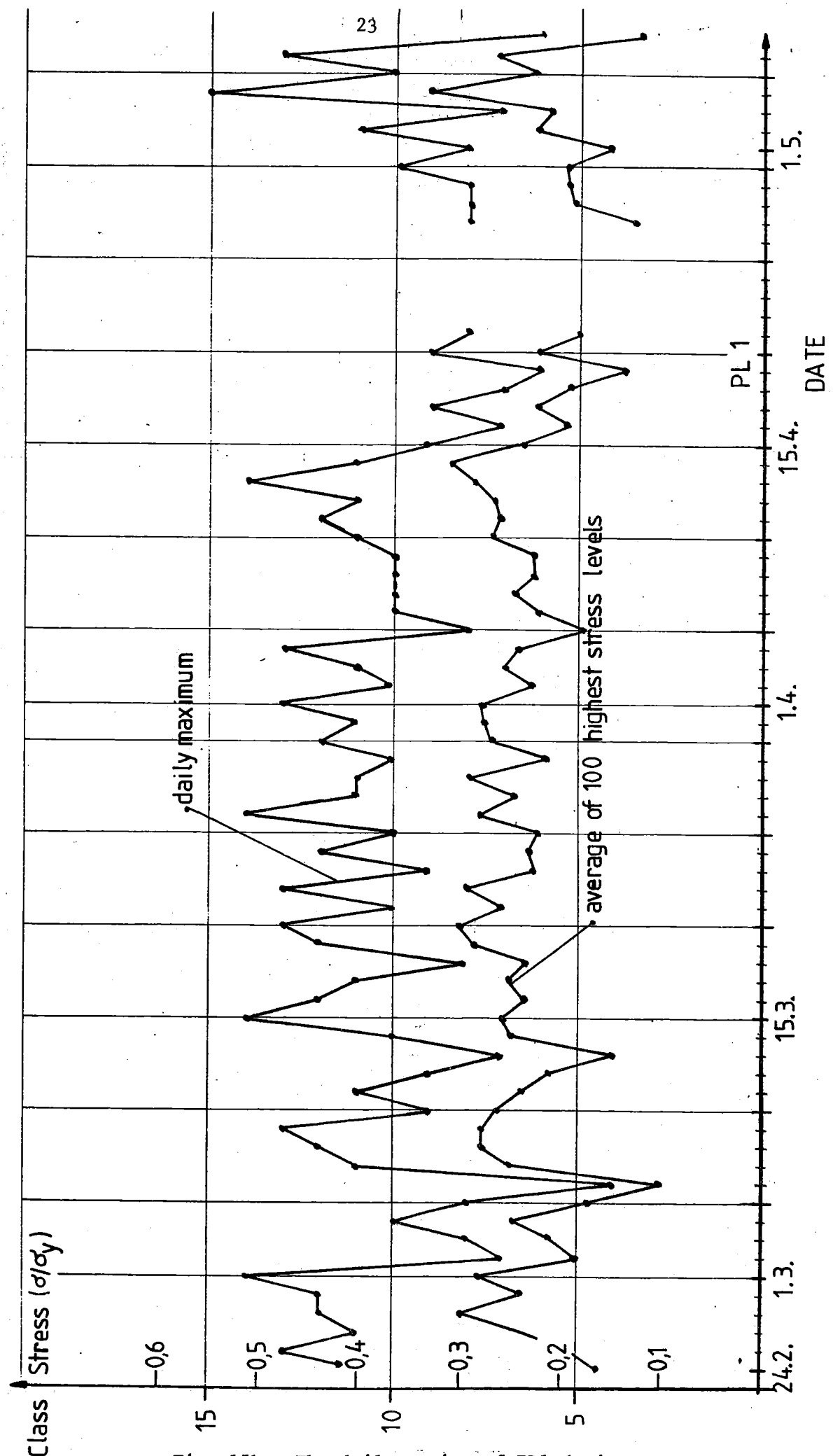

Fig. 15b. The daily maxima of PL1 during the measuring period.

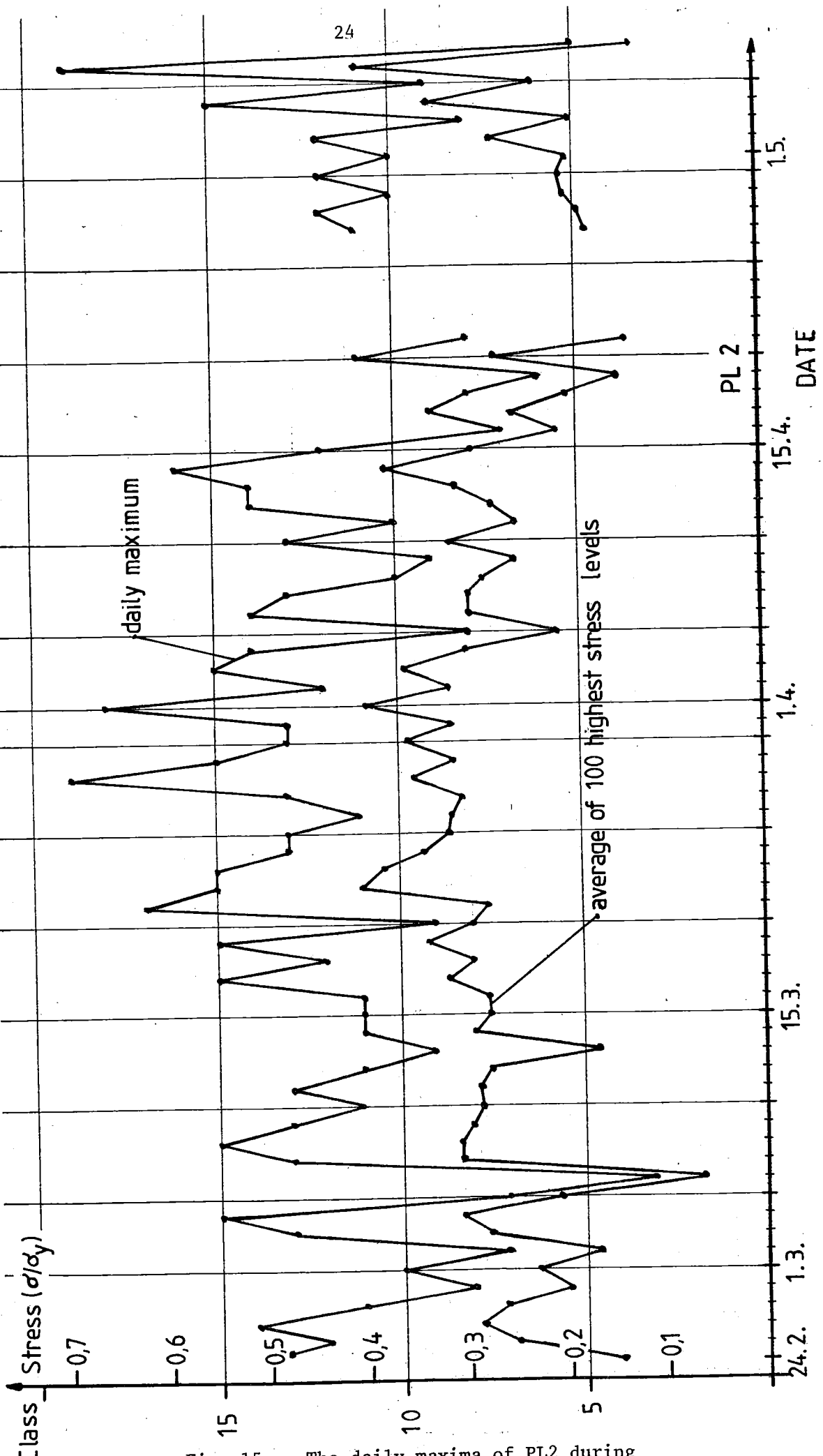

Fig. 15c. The daily maxima of PL2 during the measuring period.

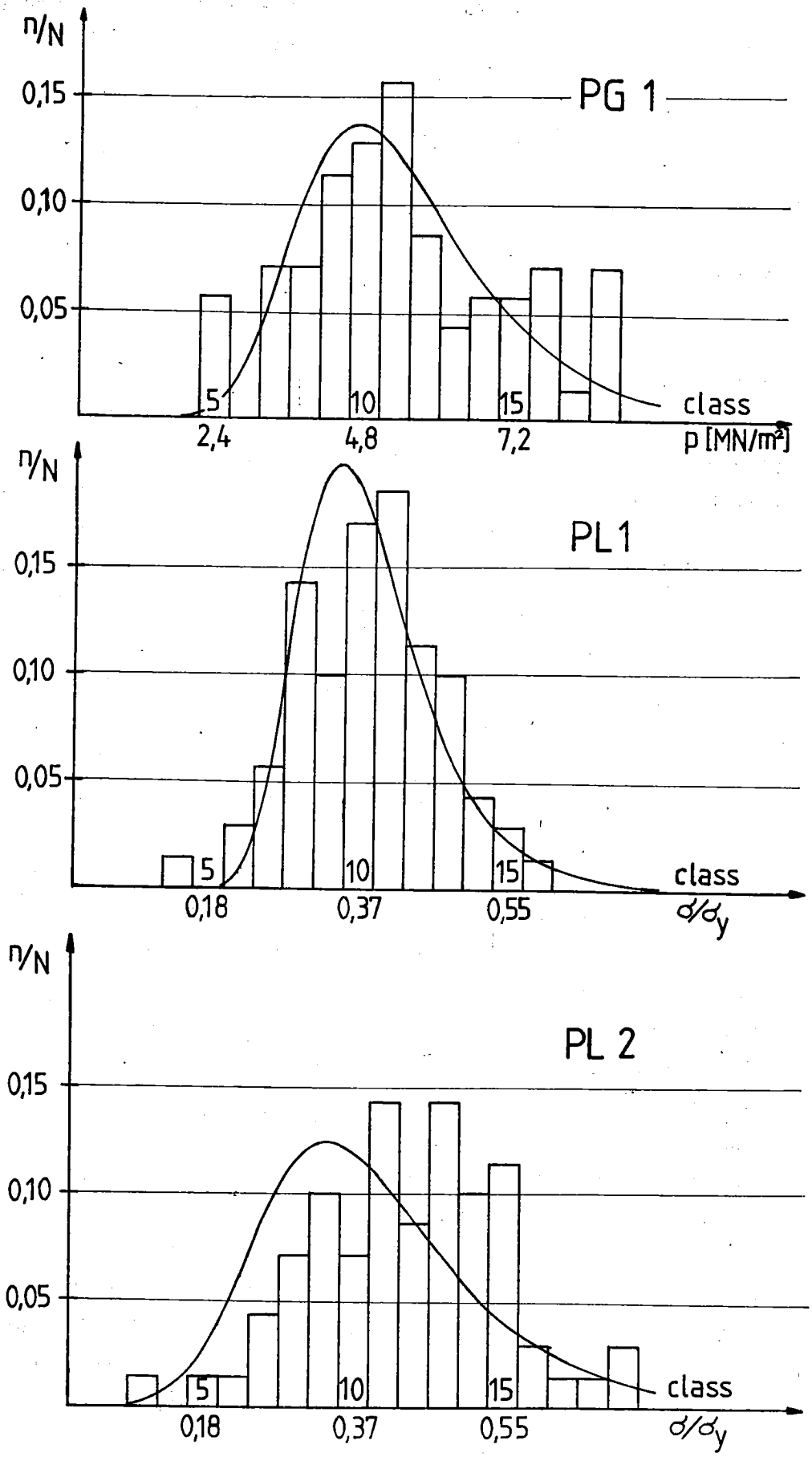

Fig. 16. The distributions of daily maxima for PG1, PL1 and PL2.

From fig. 15 the following maximum values of each channel during the whole measuring period are obtained:

PG1	$p = 86\ MN/m^2$
PL1	$\sigma/\sigma_y = 0.55$
PL2	$\sigma/\sigma_y = 0.70$

where σ_y is the yield strength.

4.2 Daily recordings

The order of stress or pressure level samples per one day is 10^7 of which by far the greatest part is in the first one or two classes. The average duration of a stress peak is about 0.3 s /8/, which means that 38 stress level samples correspond to each peak. Consequently if there is only a few samples in the highest classes, they can correspond to one single stress peak. An example of this kind of recording is shown in fig. 17a. On the other hand recordings like in fig. 17b contain many pressure peaks. All the daily recordings can be divided into those two types of daily distributions. The first type occurs quite seldom, about once in twenty days.

Before the long-term measurement commenced, the time-histories of the transducer signals were recorded for a couple of hours. From these records a view of ice pressure or stress time history can be obtained. Three samples of the time histories are presented in fig. 18. From the time histories it can be concluded that the cross-covariance of the pressure levels of the two pressure gauges is almost zero and thus there is no correlation between them. This reflects the fact that the height of ice load is quite small, and when an ice floe is bent below the hull it influences a small zone at a time. On the other hand, the cross-covariance between the output of the strain gauge and pressure gauge mounted on the same waterline (i.e. PG1 and PL4, PG2 and PL5) was nearly one at time difference which was equal to the time in which the ship travels the distance between the gauges. This reflects the fact that the ice load is quite local also in breadth and it travels along the plating.

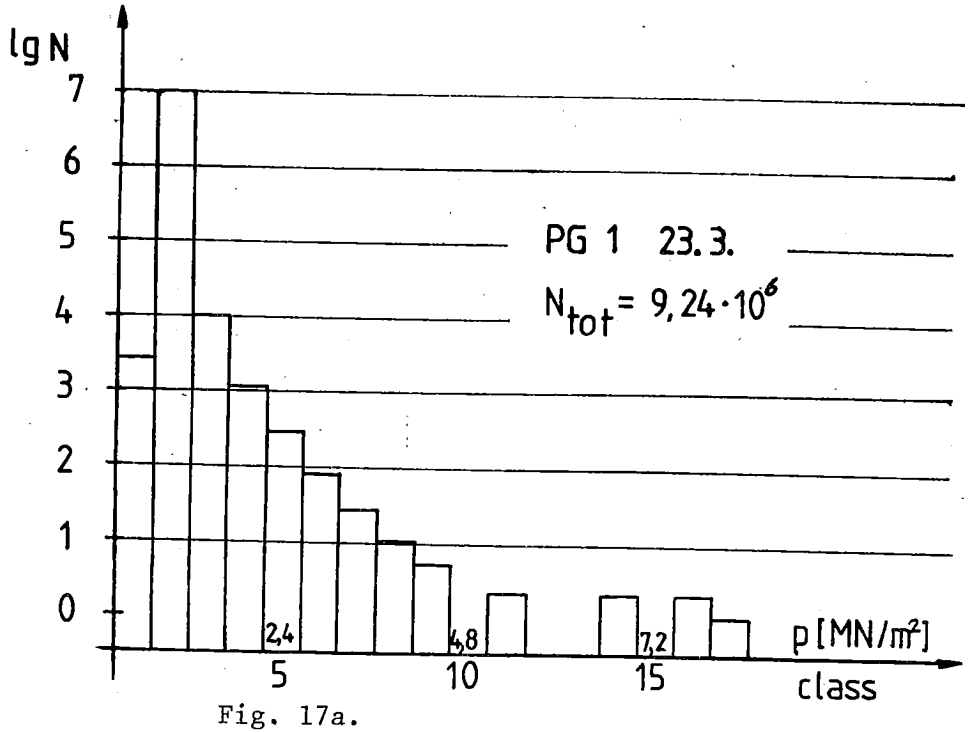

Fig. 17a.

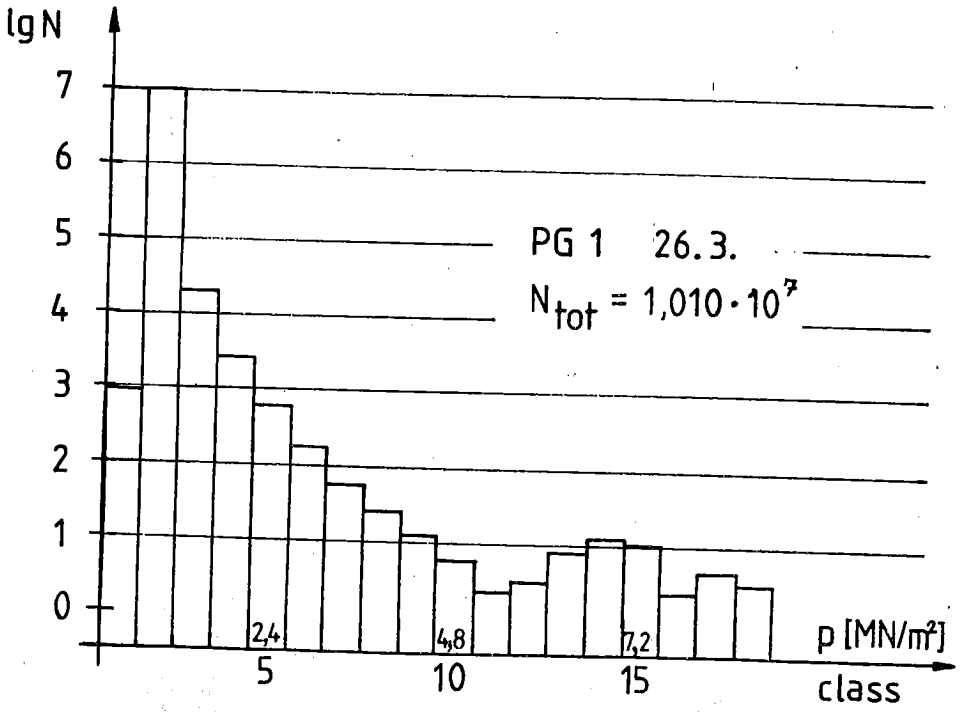

Fig. 17b.

Fig. 17. Two daily distributions of ice pressure.

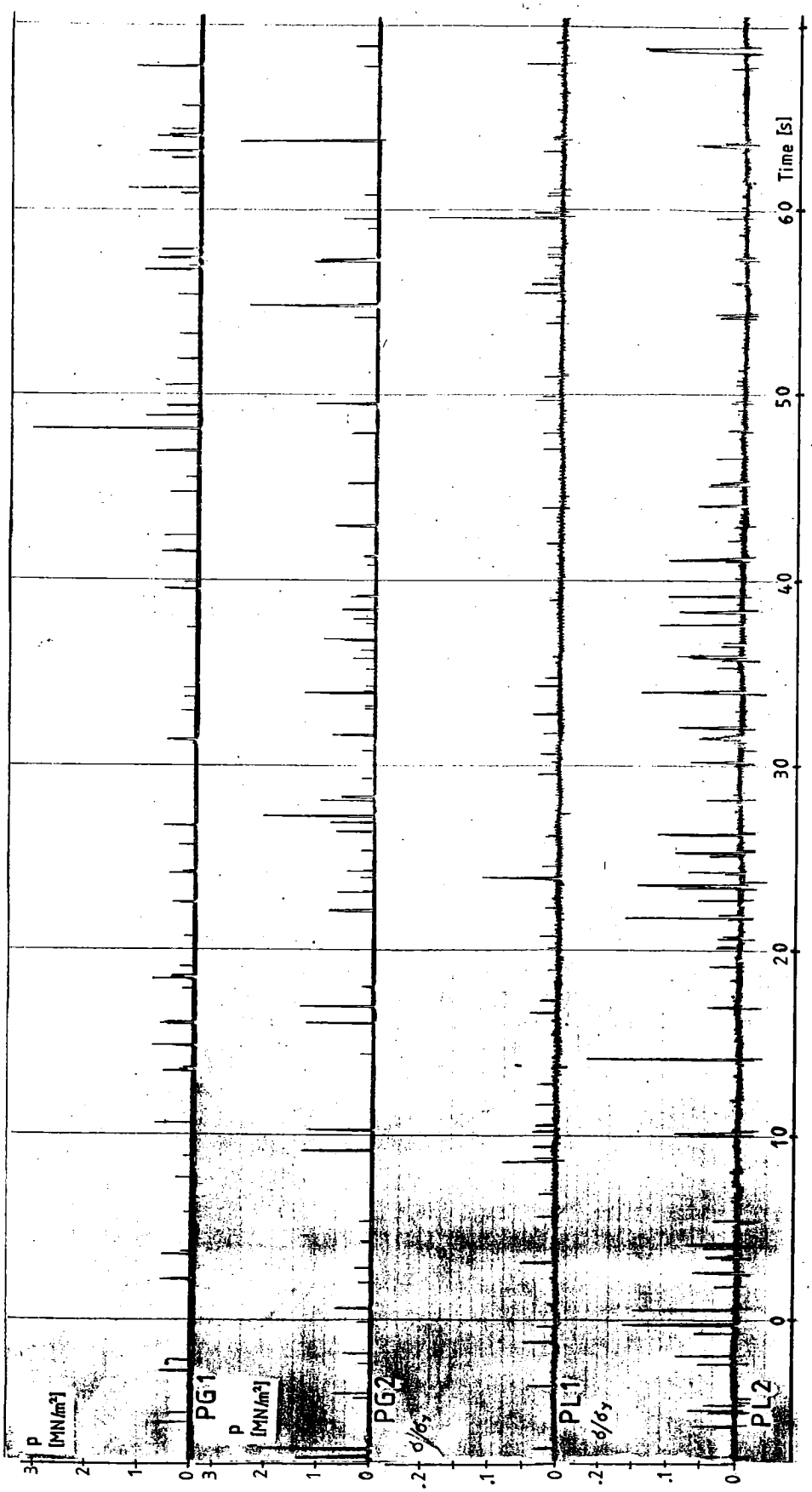

Fig. 18a. A sample of an ice pressure and stress time history.

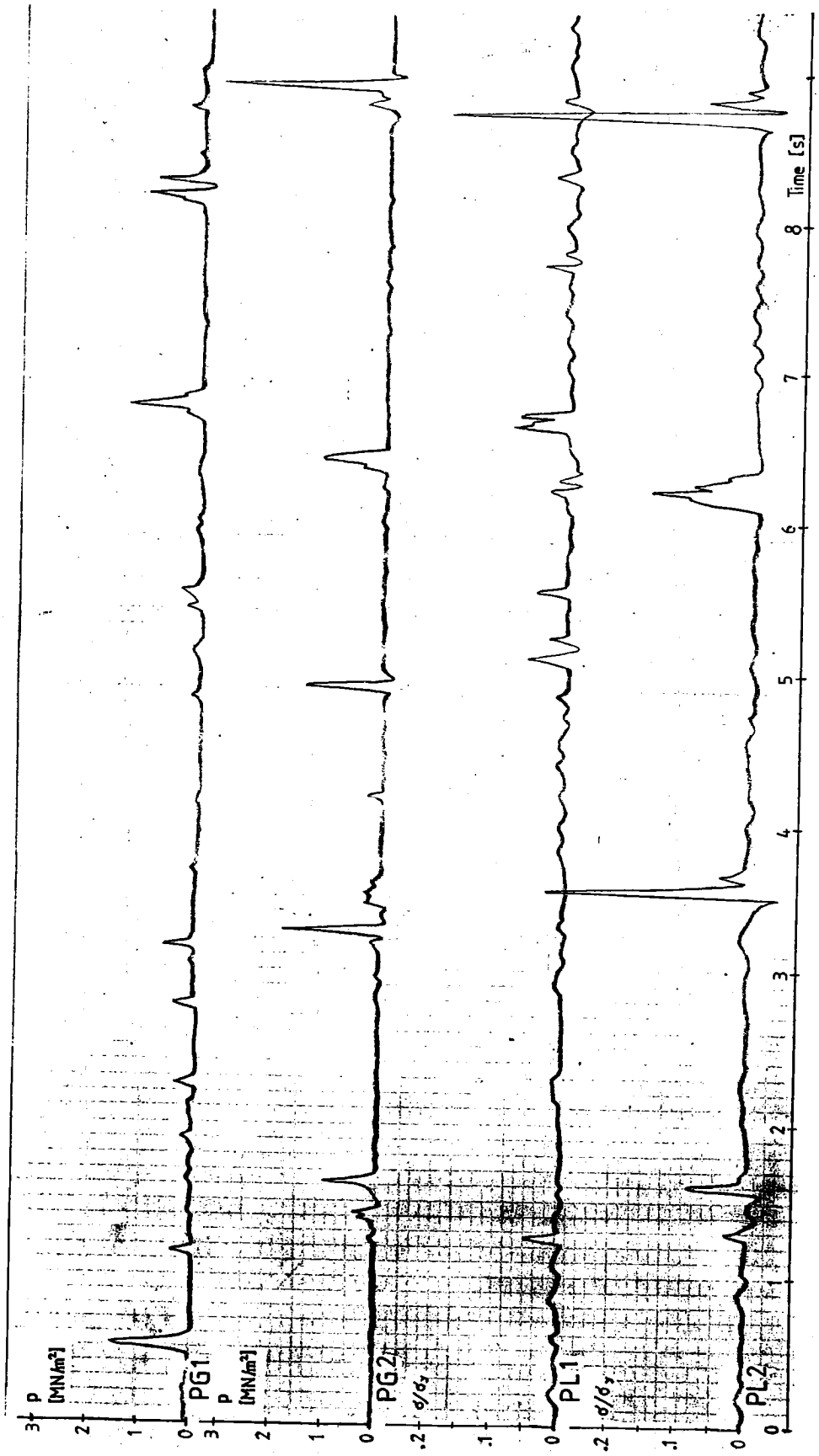

Fig. 18b. A sample of an ice pressure and stress time history.

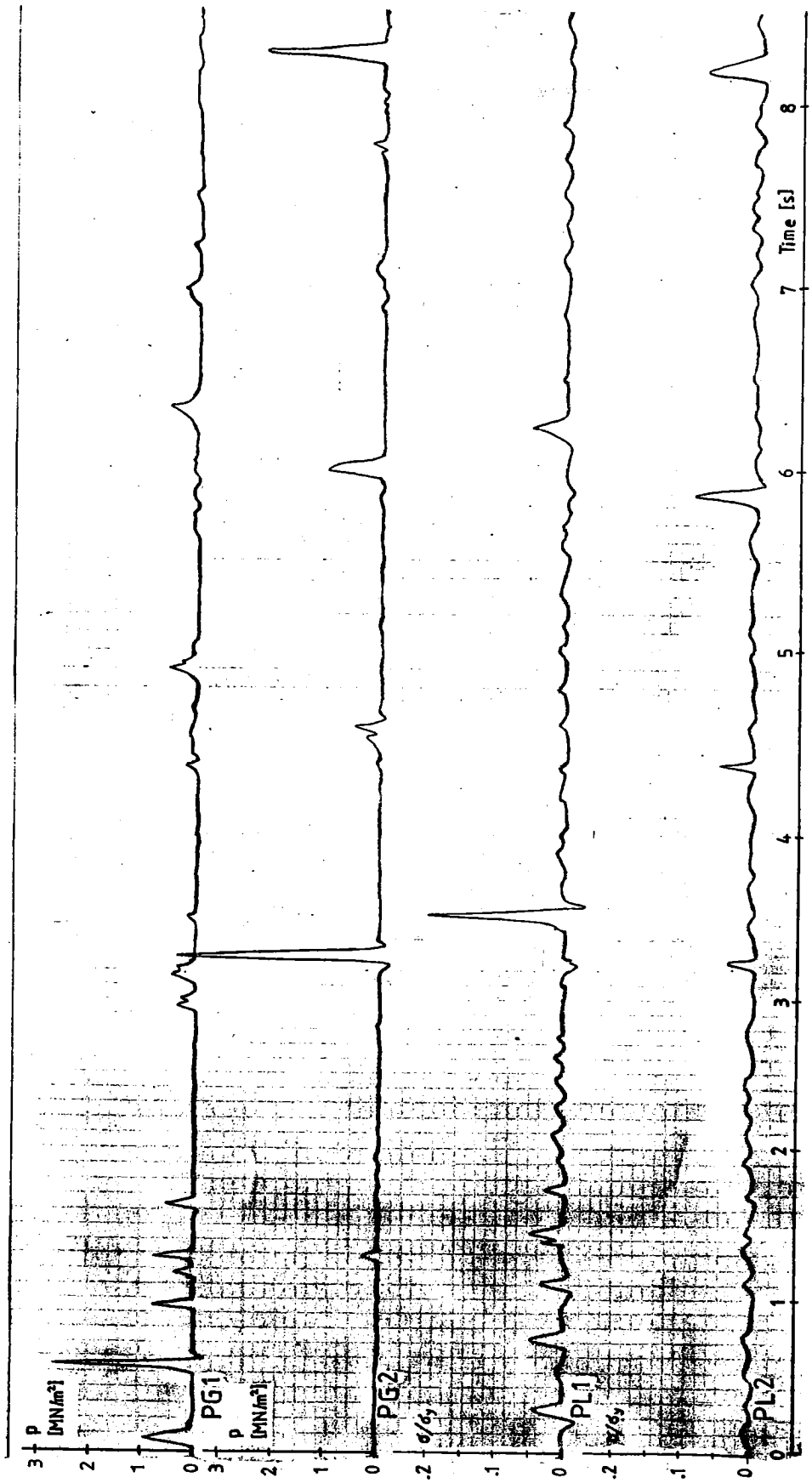

Fig. 18c. A sample of an ice pressure and stress time history.

The present daily distributions are formed from stress or pressure level samples. However, in this context, the peak amplitude distributions should be more relevant. In order to compare the output level distributions with the peak amplitude distributions, a half an hour part of the time history of PG2 was analysed. The pressure level was divided into six classes basing on the output of statistical measuring system and also manually according to pressure peaks, and thereafter the data were plotted on Weibull-probability paper, i.e., logarithm of the class number x was plotted versus ln(-ln(1-P)), where P is the probability of occurrence, fig. 19. As the points do not differ much, it can be concluded that both distributions almost completely coincide.

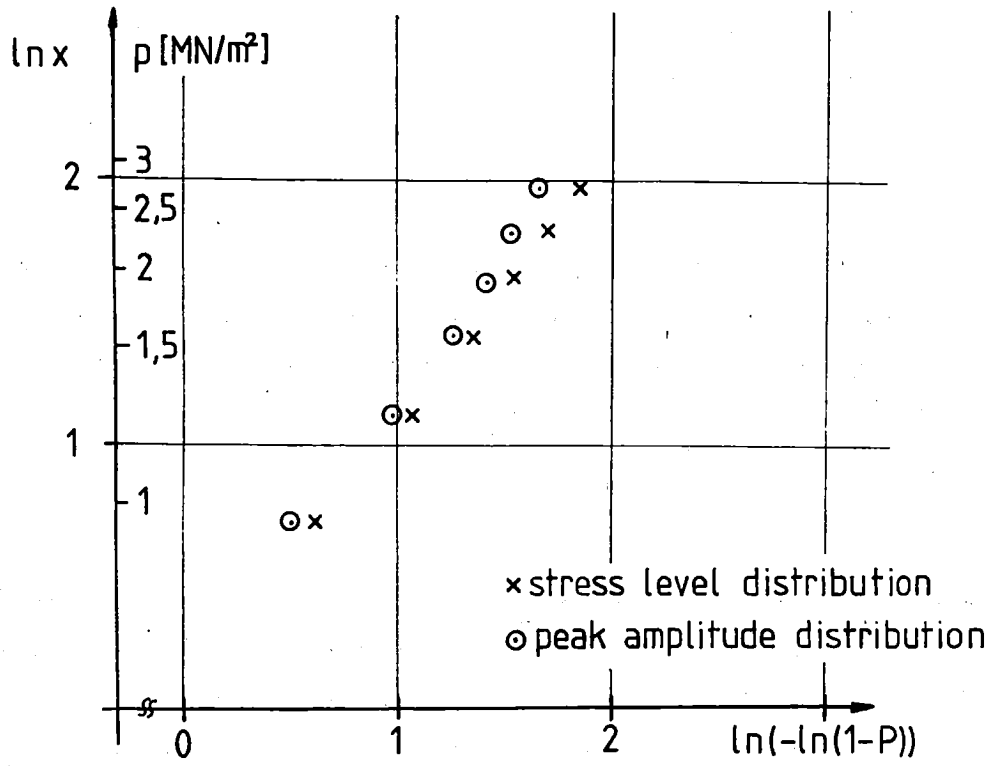

Fig. 19. A comparison of the stress level and peak amplitude distributions on Weibull-probability paper.

4.3 Statistical analysis

The object of this statistical analysis is to create reliable basis for estimation of maximum ice pressure or stress during ships life-time. There is a big scatter in the measured ice pressure values and its statistical character is clear. The size of measured sample is always finite and thus, due to the statistical nature of ice pressure, the extremal pressures must be extrapolated and examined in view of their occurrence probability. The approach here is obtained from Gumbel /3/.

The daily maxima were plotted on the Gumbel probability paper in the following way. Let the sample be in increasing magnitude $\{p_i\}$, $i = 1,\ldots,N$ where N is the total amount of daily observations. The mean frequency of mth value is

$$P(p_m) = \frac{m}{N + 1}$$

Here is the situation that the observations of the same magnitude are grouped so that the mth up to the m + kth observations are represented by a common pressure or stress value. For this reason a mean rank is attributed for each class.

$$m' = \sqrt{m(m + k)}$$

After this the observations are plotted p_m versus $-\ln(-\ln(\frac{m'}{N + 1}))$, see fig. 20a---c. In this connection the concept of return period $T(p_i)$ is important. The return period is the number of observations needed in order to obtain the value p_i. It is defined by

$$T(p_i) = \frac{1}{1 - P(p_i)} = \frac{N + 1}{N + 1 - i}$$

Also the return period is shown in fig. 20.

Fig. 20. The distributions of daily maxima plotted on Gumbel-probability paper.

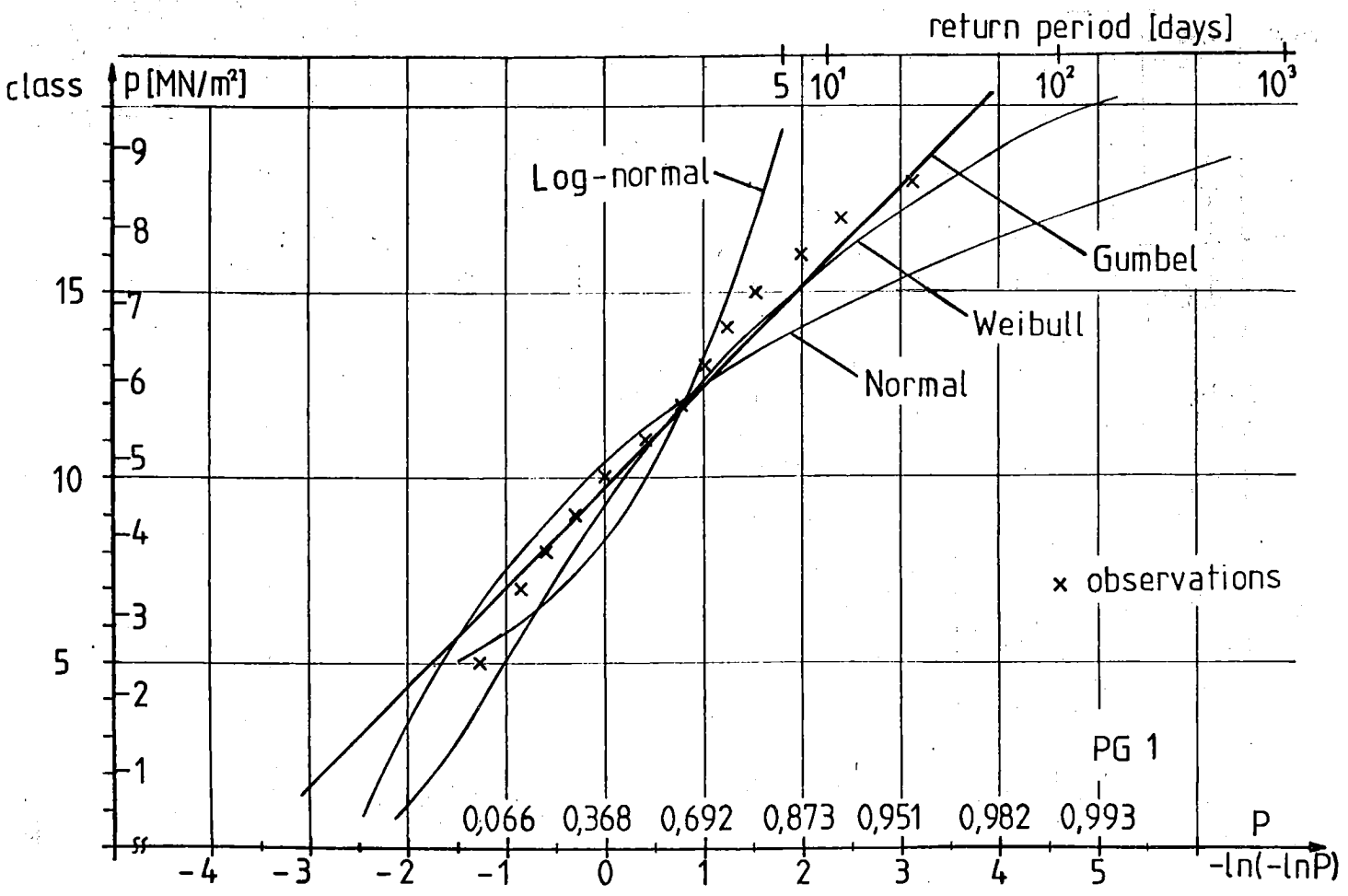

Fig. 20a. The distributions for PG1.

Fig. 20. The distributions of daily maxima plotted on Gumbel-probability paper.

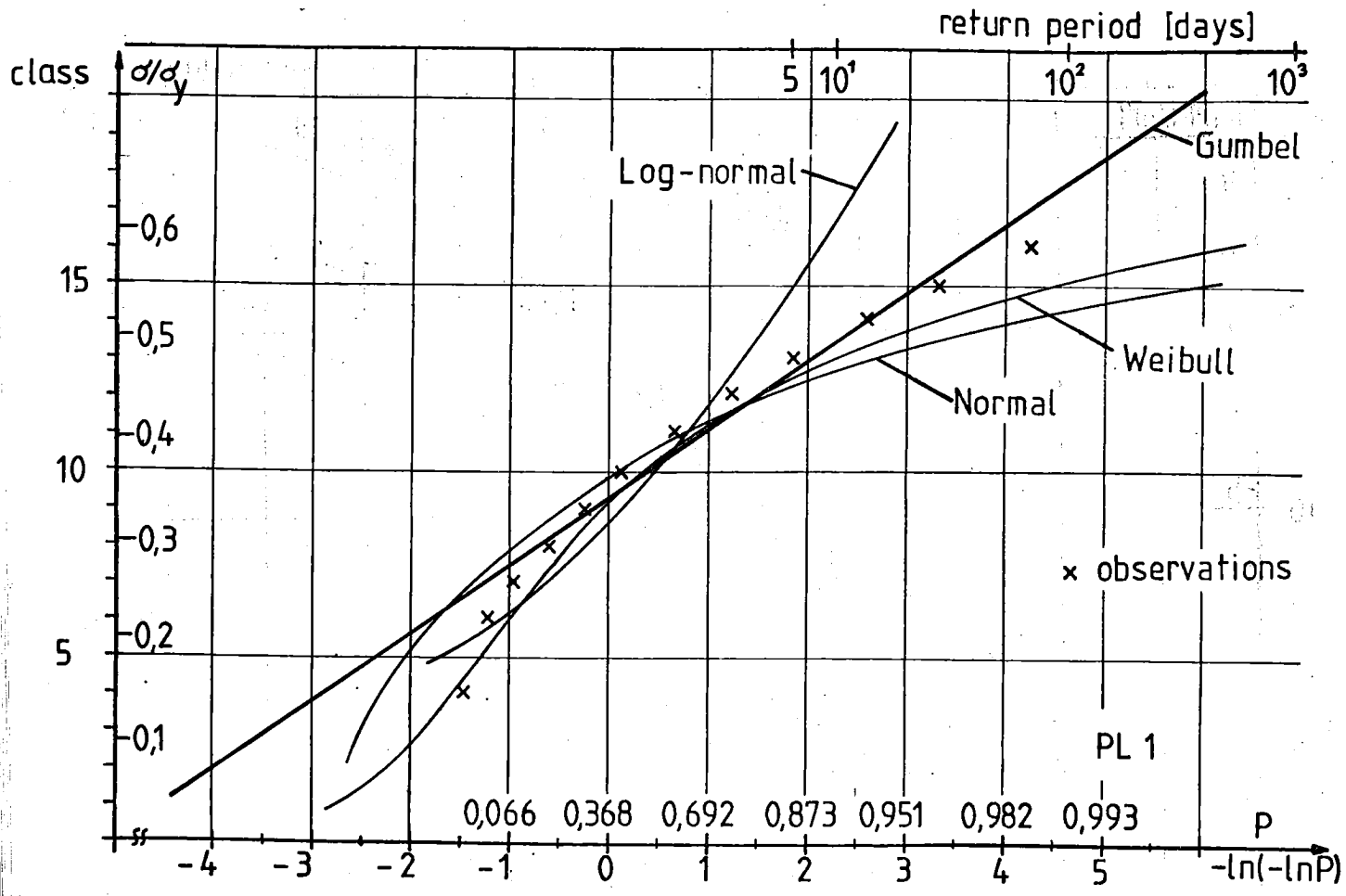

Fig. 20b. The distributions for PL 1.

Fig. 20. The distributions of daily maxima plotted on Gumbel-probability paper.

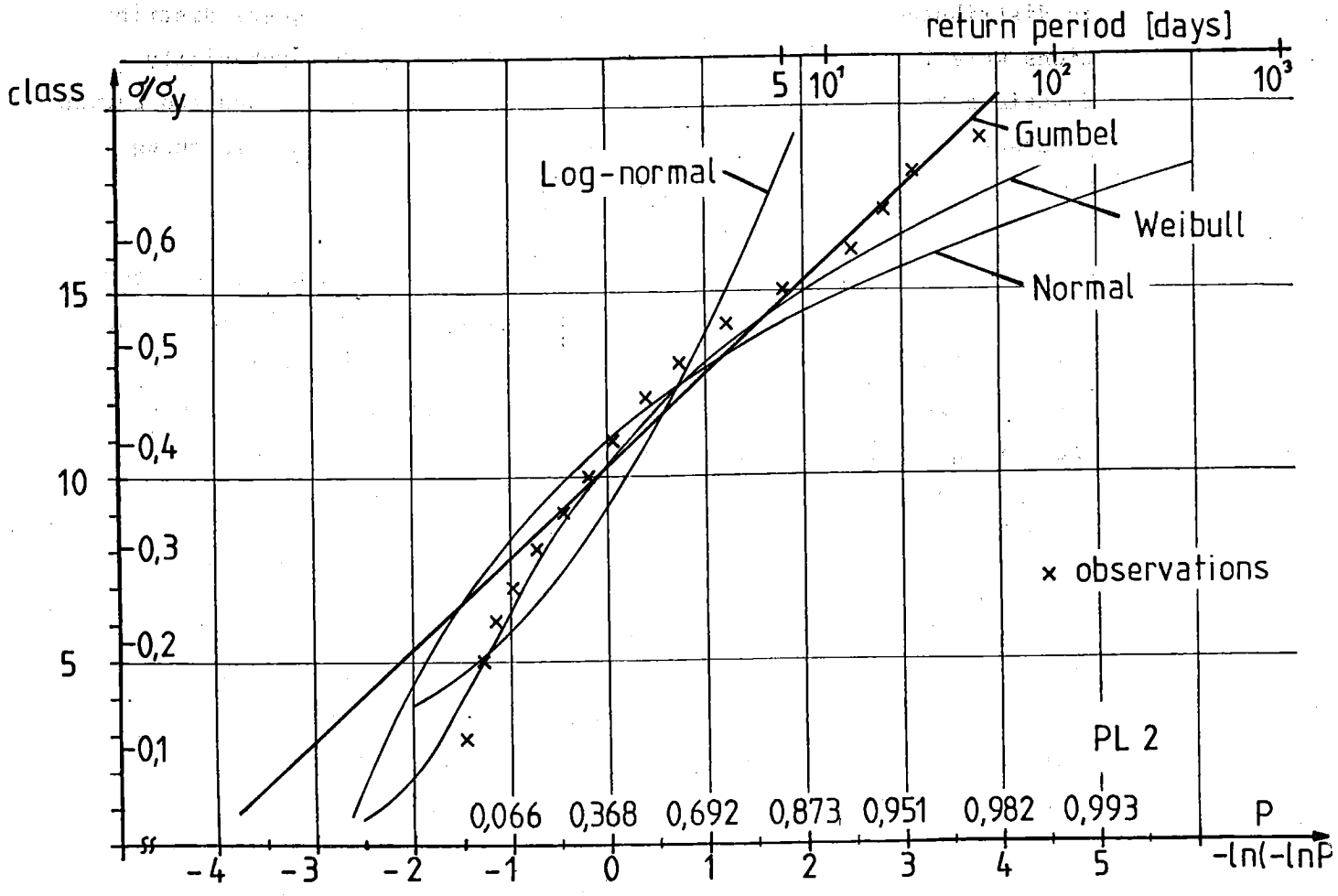

Fig. 20c. The distributions for PL2.

To be able to extrapolate to longer return periods and consequently to hither pressure or stress values it must be known how the sample is distributed. The normal, log-normal, Weibull and Gumbel distributions were fitted to the observations. After this the probability functions F(p) corresponding to each of them were determined and curves p versus $-\ln(-\ln F(p))$ were drawn in fig. 20. In table 1 is shown how the estimation of parameters was done.

Gumbel distribution fits the observations best as can be anticipated because it was created for forecasting extremes. The fit with Weibull distribution is also rather good but normal distribution gives much too long return periods and log-normal distribution gives much too short return periods. As a conclusion it can be stated that the use of Gumbel distritution for extrapolation gives the most reliable results.

The return period is an important tool in estimating the encountered stresses of pressures during the life time of a ship. At this stage of knowledge of the statistical characteristics of ice pressure the extrapolation to long time periods is doubtful due to restricted amount of observations. Still, the extrapolated values of pressure or stress corresponding to annual operating time as return period and using this value as return period the following values are obtained from fig. 20:

PG1	$p = 10.7$ MN/m
PG1	$\sigma/\sigma_y = 0.66$
PL2	$\sigma/\sigma_y = 0.80$

Table 1.

	Distribution	Probability function	Estimates of parameters
GUMBEL	$f(p) = C_1 e^{[-C_1(p-C_2)-e^{-C_1(p-C_2)}]}$	$F(p) = e^{-e^{-C_1(p-C_2)}}$	$C_1 = \frac{1,283}{S}$ $C_2 = \overline{X} - 0.577\,\frac{1}{C_1}$
WEIBULL	$f(p) = \frac{C_1}{C_2}\left(\frac{p-C_3}{C_2}\right)^{C_1-1} e^{-\left(\frac{p-C_3}{C_2}\right)^{C_1}}$	$F(p) = 1 - e^{-\left(\frac{p-C_3}{C_2}\right)^{C_1}}$	According to program presented in /1/
NORMAL	$f(p) = \frac{1}{C_1\sqrt{2\pi}}\, e^{-\frac{(p-C_2)^2}{2C_1^2}}$	$F(p) = \mathrm{erf}\left(\frac{p-C_2}{C_1}\right) = \frac{1}{C_1\sqrt{2\pi}}\int_{-\infty}^{p} e^{-\frac{(t-C_2)^2}{2C_1^2}}\,dt$	$C_1 = S$ $C_2 = \overline{X}$
LOG-NORMAL	$f(p) = \frac{e^{-\frac{1}{2C_1^2}[\ln(p-C_2)-C_3]^2}}{C_1(p-C_2)\sqrt{2\pi}}$	$F(p) = \int_{C_2}^{p} f(t)\,dt$	$C_1 = \sum_{i=1}^{N}[\ln(p_i-C_2)-C_3]^2/N$ $C_2 = \mathrm{MIN}\{p_i\}$ $C_3 = \sum_{i=1}^{N}\ln(p_i-C_2)/N$

$$\overline{X} = \sum_{i=1}^{N} p_i/N$$

$$S^2 = \frac{1}{N-1}\sum_{i=1}^{N}(p_i-\overline{X})^2$$

4.4 Influence of external conditions

The daily number of measured stress or pressure levels i.e. the size of measured sample has an influence on the highest measured stress or pressure level. Thus it should be natural to reduce the measured maxima according to the daily operation time of the icebreaker. However, the form of this reduction is of crucial importance for the reliability of the statistical analysis. As no apparent connection between the daily maxima and operation time was found (for data see appendix 1) the data used in the statistical analysis was not reduced.

Ship's speed, air temperature, ship's draft, ice thickness etc. have an effect on the theoretical ice load /5/. Air temperature and wind velocity can be obtained at four hour intervals from the logbook of the ship. No correlation between the daily maxima and temperature or wind velocity was not, however, found. This does not directly amount to that these parameters are without effect on the ice load, but that the scatter due to variations in draft, ship's speed and ice conditions eclipse their effect.

The draft of the icebreaker varies continuously when it is in operation due to the use of heeling tanks, variations in trim, pitching motions etc. The variations in draft at the location of the pressure gauges is not great so that the effect of draft variation can be neglected. Ship's speed and ice conditions are more important parameters; the recording of speed will be incorporated into this system from winter 1979, and the ice profile encountered by the icebreaker will be taken into account in the subsequent statistical analysis.

4.5 Connection between ice pressure and ice-induced stress

The local ice pressures and ice-induced stresses in the plating were studied separately in the previous chapters. The connection between these factors is now discussed. It is obvious that the spatial distribution of the load and the ice pressure itself vary greatly during the breaking process of ice edge. The only reliable method to obtain knowledge about the spatial distribution of ice load is to mount several pressure gauges close to each other both in vertical and horizontal direction.

At the short term measurements analysed in chapter 4.2, no simultaneous load on both the pressure gauges (vertical spacing 500 mm) was observed. The previous measurements /8, 9/ have also shown that when the load height is supposed to be small, the local ice pressure and ice-induced stresses in plating are incompatible if the ice load is assumed to be uniformly distributed on the loaded area. The maximum measured stresses in the plating give too low pressure values, as fig. 21 shows. On the other hand the measured maximum ice pressures give too high stress values in the plating. The connection between the measured maximum stress in the frame and the maximum ice pressure has proved almost compatible.

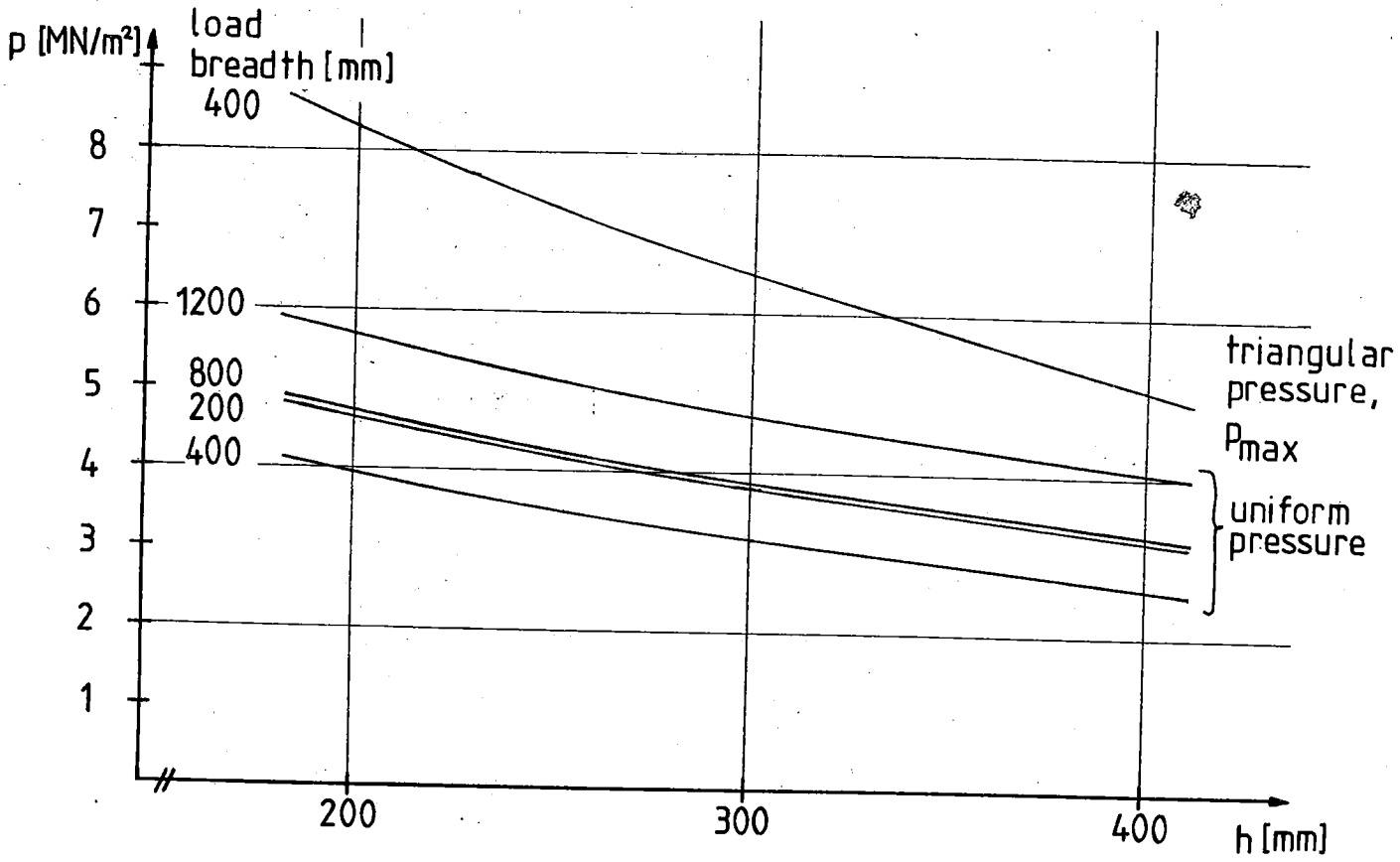

Fig. 21. The influence of load height on the calculated ice pressure with a prescribed stress in the plating.

Because the former assumption of an uniformly distributed ice pressure leads to a contradiction, a pressure distribution, which gives a good correlation between measured maximum values, has been developed. This spatial distribution is shown in fig. 22 both for plating and frame.

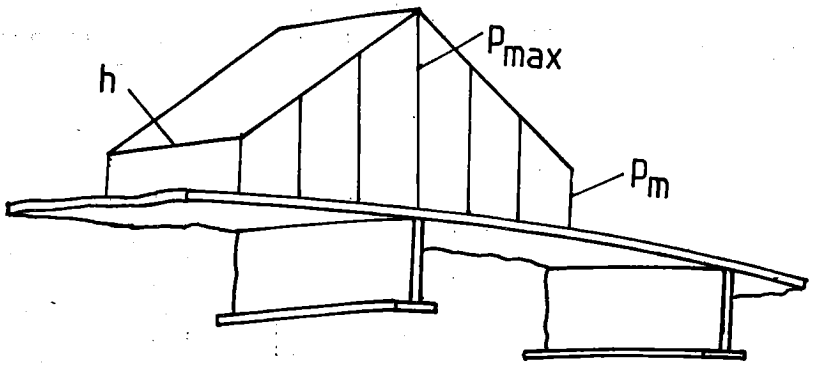

a) Load primarily on a frame

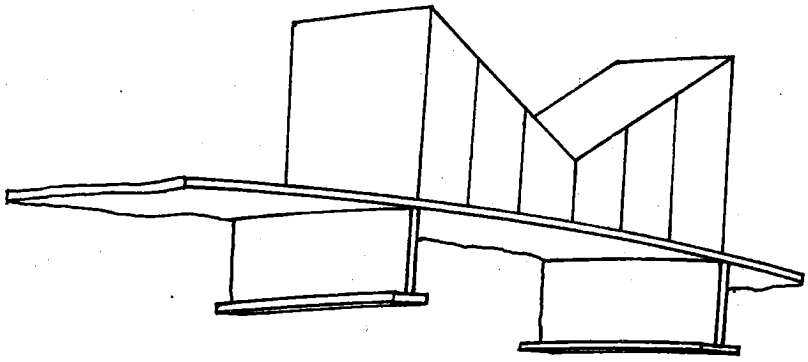

b) Load primarily on plating.

Fig. 22. The two load configurations which explain the measured stress values in frames and plating.

An intuitive explanation for the physical background of this spatial distribution is that the flexural stiffness of frame is higher than that of plating. In the case of icebreaker SISU the ratio of flexural stiffness is about ten. Consequently the stress field induced in the ice field is inhomogeneous and the distribution of the ice pressure follows the configuration shown in fig. 22. Using this kind of pressure distribution for plating with $p_{max} = 8.5$ MN/m^2 and $\sigma_{max}/\sigma_y = 0.697$, $p_m = 2.4$ MN/m^2. In this calculation the element mesh of the structure was somewhat simplified, see fig. 23. From these two pressure values the conclusion can be drawn that the value of p_{max} corresponds to the multiaxial strength of sea ice and p_m is close to the uniaxial strength of sea ice.

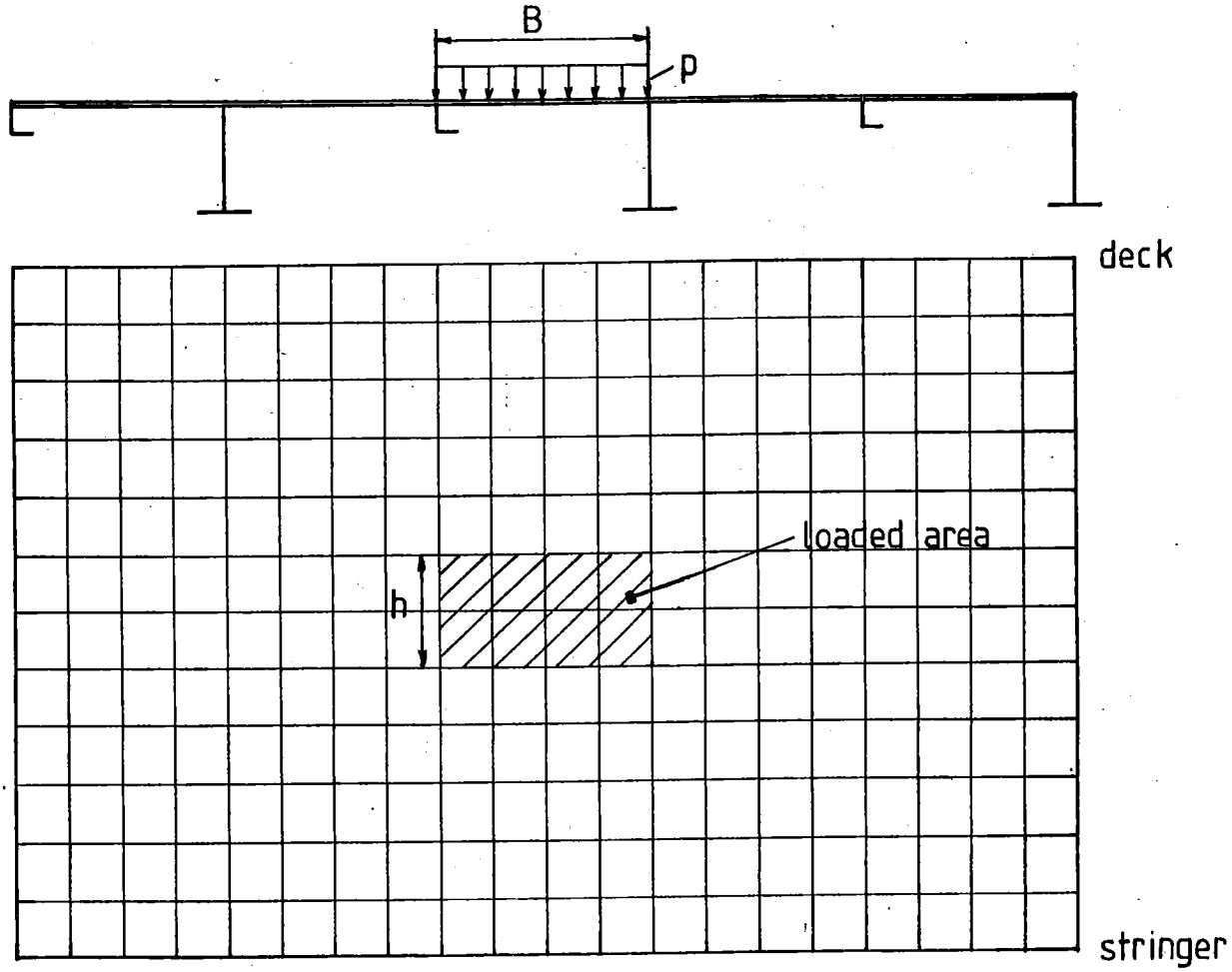

Fig. 23. Element mesh of the shell structure of the icebreaker SISU.

5. CONCLUSIONS

The most striking result of this investigation is the high value, 8.5 MN/m^2, of the local ice pressure. This value seems high because in naval architecture the ice pressure is traditionally thought to be of order of the uniaxial compressive strength of sea ice, about 3 MN/m^2 /7/. However, the stress field in the ice plate is not usually uniaxial and thus the contact pressure can be two or three times higher than the compressive strength /2/.

The statistical analysis showed that the daily maxima of pressure or stress followed quite closely the Gumbel distribution. Using this distribution and the operating time in 1978 as return period, it can be concluded that the ice pressure of 10.7 MN/m^2 and stress of 0.80 (divided with yield strength) is encountered once during a winter. The extrapolation to very high ice pressure values must be viewed somewhat critically because probably there is some ultimate maximum of ice pressure which is reached when all external conditions are perfect. This ultimate pressure must be obtained by analytical methods or by laboratory tests.

The measurements and calculations of ice-induced stresses presented here gave an indication that the form of ice pressure is not uniform. The discrepancy between measured stresses in frames and plating can be explained if the ice pressure is of saw tooth form. Thus the flexibility of ship's side has an effect on the value of design ice pressure.

On the basis of these measurements and results it is felt that this kind of statistical approach gives the most reliable design ice pressures and loads.

ACKNOWLEDGEMENTS

This study was finacially supported by the Winter Navigation Research Board in Finland and Sweden. We want to express here our gratitude for the financial support. We also want to thank Mr. Vuorinen from the Electrical Engineering Laboratory of the Technical Research Centre of Finland for programming the microprocessor unit in the statistical measuring system.

Without close cooperation with the Finnish Board of Navigation and the crew of icebreaker SISU this study would not have been possible. Thus we take the opportunity here to express our warmest gratitude for the flexibility offered in arrangements and for the helpful atmosphere onboard.

REFERENCES

/1/ Askren W.B. — Mathematical modelling of human performance errors for reliability analysis of system. Aerospace medical research laboratory, Ohio 1969.

/2/ Croasdale K.R. — Ice forces on fixed rigid structures. A report prepared for the working group on ice interaction on hydraulic structures, committee on ice problems, International Association for Hydraulic Research. April 1978, 61 p.

/3/ Gumbel E.J. — Statistics of extremes. Columbia University Press, New York 1958, 375 p.

/4/ — Kuukausikatsaus Suomen ilmastoon (monthly review of Finnish climate) Vol 72, February - May, 1978.

/5/ Major R.A. & Berenger D.M. & Lawrie C.J. — A model to predict hull-ice impact loads in the St. Lawrence. Ice Tech symposium, Montreal, Canada, April 9-11. 1975. pp. D-1...D-33.

/6/ Palosuo E.A. — A treatise on severe ice conditions in the central Baltic. Report no. 156 of the Institute of Marine Research. Helsinki 1953, 130 p.

/7/ Ruck K.-W. & Freund H. — Festigkeiten von Ostsee- und Süsswasser Eis. Der Bauingenieur, 44(1969) Heft 9, pp. 339-343.

/8/ Varsta P. — Measurement and analysis of ice-induced stresses in the shell of an icebreaker. Winter Navigation Board, research report no. 21, Helsinki and Stockholm 1977.

/9/ Varsta P. and Vuorio J. — Analysis of ice-induced loads and structural responses of the shell of mt. IGRIM during ice trials in 1978. VTT Ship Laboratory, research report A 9172/78, (unpublished).

Date	PG1	PL1	PL2	Mean wind speed (m/s)	Mean temp. (°C)	Distance (nautical miles)	Operating time (h)	Mean speed (knots)	Approximate route
	CLASS								
24.2.	10	11	14	16.3	- 8.5	171	21.1	8.1	Kemi - Helsingkallan
25.2.	7	13	11	11.3	- 1.3	271	22.3	12.1	Kallan - - Utgrynnen
26.2.	15	11	14	10.3	0.7	271	24.0	11.3	Ensten - Kallan - Tankar - Kemi - Oulu
27.2.	16	12	11	10.2	0.2	206	21.1	9.8	Oulu - Nahkiainen - Tankar - Nordvalen - - Utgrynnen
28.2.	10	12	8	8.5	0.2	263	22.8	11.5	Sydostbrotten - - Kemi
1.3.	13	15	10	7.2	1.0	167	15.8	10.6	Kemi - Oritkari - Virpiniemi
2.3.	9	7	7	2.5	1.0	137	12.8	10.7	Virpiniemi - Kraasukka - Ajos - - Keminkraaseli - Kemi
3.3.	16	8	13	5.5	1.2	238	21.0	11.3	Kemi - Nordvalen - Kallan - Nordvalen
4.3.	15	10	15	9.2	1.0	228	24.0	9.5	Sydstbrotten - - Oulu
5.3.	9	8	7	10.0	0.5	100	10,0	10.0	Oulu - - Vihreäsaari
6.3.	5	4	3	8.5	1.5	11	2.0	5.5	——
7.3.	9	11	13	10.3	- 0.5	233	24.0	9.7	Oulu - Nordvalen - Kallan
8.3.	7	12	15	5.8	- 1.5	235	24.0	9.8	Ulkokalla - Oulu - Kemi
9.3.	16	13	14	8.7	- 1.2	256	24.0	10.7	Kraasukka - Oulu - Tankar - Nahkiainen

10.3.	9	9	11	11.0	0.5	200	21.7	2.2	Marjaniemi - Kemi - Kraasukka - Ulko-krunni - Ajos
11.3.	8	11	13	12.2	- 1.5	198	18.0	11.0	Ajos - Nahkiainen - Bjuröklubb - - Nordvalen
12.3.	7	9	11	8.2	- 1.3	150	1.50	10.0	Nordvalen - Ulkokalla - Tankar - Nordvalen
13.3	5	7	9	9.8	- 0.2	54	3.9	13.8	Nordvalen - Norrskär - Utgrynnen
14.3.	9	10	11	16.3	- 7.7	195	24.0	8.1	Nordvalen - Tankar - Kallan - - St Fjäderägg
15.3.	8	14	11	11.0	-10.8	205	24.0	8.5	Jägarören - - Nahkiainen
16.3.	12	12	11	7.0	-12.5	160	18.2	8.8	Marjaniemi - Vihreäsaari - Nahkiainen
17.3.	16	11	16	6.0	-11.2	196	23.2	8.5	Nahkiainen - Tankar - Mässkär - - St Fjäderägg - Nordvalen
18.3	10	8	12	15.2	-11.3	240	24.0	10.0	Kallan - St Fjäderägg - Kallan - - St Fjäderägg
19.3.	11	12	15	7.2	-11.5	217	19.5	11.1	Yxpila - Kallan - Tankar - Ulkokalla
20.3.	10	13	9	5.8	-12.0	160	16.4	9.7	Nahkiainen - Oulu - Oritkari - Raahe
21.3.	13	10	17	6.0	-12.0	201	22.8	8.8	Nahkiainen - Ulkokalla - Marjaniemi - - Oulu - Vihreäsaari
22.3.	10	13	15	4.8	-12.0	176	21.3	8.3	Virpiniemi - Ajos - Oulu - Marjaniemi
23.3	16	9	15	5.2	- 9.5	192	23.0	8.3	Marjaniemi - - Nordvalen
24.3.	8	12	13	10.2	- 6.3	235	24.0	9.8	St Fjäderägg - Kokkola - St Fjäderägg - - Ulkokalla - Raahe
25.3.	9	10	13	11.0	0.5	222	24.0	9.3	Nahkiainen - - Nordvalen

26.3.	17	14	11	11.5	1.7	273	24.0	11.4	Nordvalen - Raahe - Nordvalen
27.3.	11	11	13	9.0	1.5	282	24.0	11.8	Helsingkallan - Ulkokallan - Nahkiainen - - Ulkokalla - Nordvalen - Kallan
28.3.	11	11	19	8.3	2.5	178	21.0	8.5	Kallan - Oulu - Virpiniemi
29.3.	14	10	15	8.0	2.2	106	10.0	15.6	Virpiniemi - Ulkokalla
30.3.	10	12	13	132.	2.5	266	24.0	11.1	Tankar - Nordvalen - Raahe - Ulkokalla
31.3.	12	11	13	9.5	2.0	229	19.5	11.7	Tankar - St Fjäderägg - Ajos
1.4.	14	13	18	7.5	0.2	195	24	8.1	Kraasukka - Bjuröklubb - Nahkiainen
2.4.	10	10	12	7.5	- 1.5	141	17	8.3	Nahkiainen - Raahe - Nahkiainen
3.4.	10	11	15	5.2	- 2.8	228	20	11.4	Nahkiainen - Oritkari - Nahkiainen
4.4.	18	13	14	4.7	- 3.2	157	12.7	12.4	Nahkiainen - Raahe - Ulkokalla
5.4.	9	8	8	6.8	- 1.2	226	20.7	10.9	St Fjäderägg - Nahkiainen - St Fjäderägg
6.4.	9	10	14	13.2	1.3	261	24.0	10.9	Norrskär - Kallan - Nahkiainen - Bjuröklubb
7.4.	18	10	13	9.3	1.0	257	24.0	10.7	Nygrän - Norströmsgrund - Bjuröklubb - - Ulkokalla - Raahe - Ulkokalla - - Bjuröklubb
8.4.	11	10	10	4.8	1.2	260	21.3	12.2	Nahkiainen - Raahe - Kalla - Raahe
9.4.	12	10	9	10.3	1.7	84	11.3	7.5	Raahe - Ulkokalla - Nahkiainen
10.4.	11	11	13	8.8	0.2	131	12.4	10.6	Nahkiainen - Oulu - Vihreäsaari
11.4.	18	12	10	6.8	1.0	240	24.0	10.0	Vihreäsaari - Kemi - Bjuröklubb - Nahkiainen
12.4.	11	11	14	10.0	2.3	211	22.4	9.4	Nahkiainen - Bjuröklubb - Marjaniemi - Oulu

13.4.	15	14	14	15.0	1.7	198	23.8	8.3	Oulu - Nahkiainen - Bjuröklubb
14.4.	15	11	16	14.3	1.2	196	22.4	8.8	Nahkiainen - Oulu - Ajos - Kraasukka
15.4.	11	9	12	7.2	2.5	141	14.1	10.0	Ajos - Oulu
16.4.	7	7	7	12.3	0.3	133	10.5	12.7	Mahkiainen - Bjuröklubb - Nahkiainen
17.4.	14	9	9	14.0	- 1.7	273	24.0	11.4	Marjaniemi - Kemi - Marjaniemi - - Bjuröklubb - Nahkiainen - Marjaniemi
18.4.	11	7	8	9.3	- 1.0	49	5.9	8.3	Kemi
19.4.	5	6	6	1.5	- 1.5	18	2.0	9.0	Kemi
20.4.	11	9	11	2.0	- 0.7	73	8.7	8.4	Kemi - Vihreäsaari - Oulu
21.4.	12	8	8	0.7	1.0	24	2.9	8.2	Oulu -
27.4.	12	8	11	5.7	- 0.8	74	7.0	10.6	Oulu - Ajos
28.4.	12	8	12	6.2	- 2.0	124	11.0	11.3	Ajos - Oulu
29.4.	8	8	10	4.8	- 1.5	11	1.1	10.2	Oulu
30.4.	11	10	12	7.0	0.0	78	5.6	14.0	Oulu - Ulkokalla
1.5.	14	8	10	5.8	1.5	162	12.3	13.1	Ulkokalla - Kemi
2.5.	11	11	12	1.7	1.7	61	6.0	10.2	Kemi - Oulu 1
3.5.	10	9	8	6.2	1.2	149	12.0	12.4	Oulu 3 - Kemi - Tankar - Ulkokalla
4.5.	18	15	15	7.5	2.5	235	18.8	12.5	Nahkiainen - Tankar - Ulkokalla - - Nahkiainen

5.5.	8	10	9	5.8	1.2	152	12.6	12.1	Nahkiainen - Tankar - Nahkiainen - Ulkokalla
6.5.	13	13	19	2.0	1.5	229	20.7	11.1	Tankar - Nahkiainen - Tankar - Rata - Storgrund
7.5.	5	6	5	5.2	2.0	88	7.0	12.6	Rata Storgrund - Tankar - St Fjäderägg
8.5.	18	16	9	8.0	1.7	162	11.8	13.7	Rata Storgrund - Tankar - Nahkiainen - Tankar - - St Fjäderägg

SWEDISH/FINNISH WINTER NAVIGATION

RESEARCH BOARD

R E P O R T S

No. Titel

1. HAVSINSKONFERENS. Protokoll (1972).

2. VINTERSJÖFART I BOTTENHAVET - Erfarenheter av SCA:s distributionssystem - L. Sjöstedt och S. Hammarsten (1972).

3. ISSKADOR PÅ FARTYG I ÖSTERSJÖN, BOTTENHAVET OCH BOTTENVIKEN. - Statistisk analys av skadefrekvenser - L. Sjöstedt och S. Hammarsten (1973).

4. PROPELLERPROBLEM. Propellerverkningsgradens beroende av bladutformningen. H. P. Loid (1973).

5. FARTYGS FRAMDRIVNINGSMOTSTÅND I IS. E. Enkvist (1974).

6. VINTERSJÖFART MED STORA FARTYG I BOTTENVIKEN - Rapport av en arbetsgrupp (1974).

7. VINTERSJÖFART I BOTTENVIKEN. Symposium Luleå (1974).

8. HAVSISUNDERSÖKNINGEN I BOTTENVIKEN VINTERN 1974. A. Omstedt, T. Thompson och I. Udin (1974).

9. KARTERING AV YTVATTENTEMPERATUREN I VATTNEN RUNT SVERIGE. J-E. Lundqvist, A. Omstedt och I. Udin (1974).

10. EXPERIMENTS ON REMOTE SENSING OF SEA ICE USING A MICROWAVE RADIOMETER. M. Tiuri, M. Hallikainen and K. Kaski (1974).

11. BOTTENVIKENS STÅLFYRAR - HÅLLFASTHETSANALYS OCH FÖRBÄTTRINGSFÖRSLAG. M. Määttänen (1974).

12. FORMATION AND STRUCTURE OF ICE RIDGES IN THE BALTIC. E. Palosuo (1975).

13. CALCULATION OF ICE DRIFT IN THE BOTHNIAN BAY AND THE QUARK. A. Valli and M. Leppäranta (1975).

14. A. NARROW BEAM SONAR TO MEASURE THE SUBMARINE PROFILE OF AN ICE RIDGE. E. Palosuo, T. Pousi and M. Luukkala (1976).

15. THW AVERAGE SURFACE TEMPERATURE IN THE AUTUMN AND THE EARLY WINTER ON THE GULF OF BOTHNIA, THE NORTHERN BALTIC SEA AND THE GULF OF FINLAND (1966-1974). H. Grönvall and E. Palosuo (1976).

16:1 SEA ICE -75. Programme. Å. Blomquist, C. Pilo and T. Thompson (1975).

16:2 SEA ICE -75. Ground truth report. I. Udin (1976).

16:3 SEA ICE -75. Ice detection by SLAR. R. H. J. Morra and G. P. de Loor (1976).

16:4 SEA ICE -75. Analysis of SLAR data. S. Parashar (1976).

16:5 SEA ICE -75. FLAR, ODAR, ship's radar. J. Nilsson, T. Hagman and Y. Nilsson (1976).

16:6 SEA ICE -75. IR-scanner results. E. Fagerlund and G. Lundholm (1976).

16:7 SEA ICE -75. Radaraltimeter results. S. Axelsson (1976).

16:8 SEA ICE -75. Dynamical report. I. Udin and A. Omstedt (1976).

16:9 SEA ICE -75. Summary report. Å. Blomquist, C. Pilo and Thompson (1976).

17. THE SHAPE AND SIZE OF ICE RIDGES IN THE BALTIC ACCORDING TO MEASUREMENTS AND CALCULATIONS. Arno Keinonen (1976).

18. A NUMERICAL MODEL FOR FORECASTING THE ICE MOTION IN THE BAY AND SEA OF BOTNIA. I. Udin and A. Ullerstig (1977).

19. CREEP OF FRESH WATER ICE AT HIGH HOMOLOGOUS TEMPERATU[illegible]S. E. K. M. Leppävuori (1976).

20. ECONOMICS OF WINTER NAVIGATION IN THE NORTHERN PART OF THE GULF OF BOTNIA. B. M. Johansson (1977).

21. MEASUREMENT AND ANALYSIS OF ICE-INDUCED STRESSES IN THE SHELL OF AN ICEBREAKER. P. Varsta (1977).

22. MEASUREMENTS OF PHYSICAL CHARACTERISTICS OF RIDGES ON APRIL 14 AND 15, 1977. A. Keinonen (1977).

23. ICE ACCRETION ON SHIPS WITH SPECIAL EMPHASIS ON BALTIC CONDITIONS. I-E. Lundqvist and I. Udin (1978).

24. PRESENTATION OF SEA ICE RIDGES IN GENERAL AND PHYSICAL CHARACTERISTICS OF BALTIC RIDGES FOR SHIP RESISTANCE CALCULATIONS. A. Keinonen (1978).

25. ON CONDITIONS FOR THE RISE OF SELF-EXCITED ICE-INDUCED AUTONOMOUS OSCILLATIONS IN SLENDER MARINE PILE STRUCTURES. M. Määttänen (1978).

26. SOME RESULTS FROM A JOINT SWEDISH-FINNISH SEA ICE EXPERIMENT, MARCH 1977. A. Omstedt and J. Sohlberg (1978).

27. ON PLASTIC DESIGN OF AN ICE-STRENGTHENED FRAME. P. Varsta, I.V. Droumev and M. Hakala (1978).

187903552W/VAPK

ISBN 951-46-3979-0